Electronic Supplementary Material (ESI) for Inorganic Chemistry Frontiers.

Electronic Supplementary Information (ESI)

The missing MIL-101(Mn): geometrically guided synthesis and topologically correlated valence states

Yonghong Xiao,[a] Mian Li,*[ab] Jian-Rui Chen,[a] Xin Lian,[ac] Yong-Liang Huang[d] and Xiao-Chun Huang*[ab]

a Y. Xiao, M. Li, J.-R. Chen, X. Lian, Prof. X.-C. Huang
Department of Chemistry and Key Laboratory for Preparation and Application of Ordered Structural Materials of Guangdong Province, Shantou University
Guangdong 515063 (China)
E-mail: mli@stu.edu.cn, xchuang@stu.edu.cn

b M. Li, Prof. X.-C. Huang
Chemistry and Chemical Engineering Guangdong Laboratory
Shantou 515031 (China)

c X. Lian
School of Materials Science and Engineering, National Institute for Advanced Materials, TKL of Metal and Molecule-Based Material Chemistry, Nankai University
Tianjin 300350 (China)

d Y.-L. Huang
Department of Medicinal Chemistry, Shantou University Medical College
Shantou, Guangdong 515041 (China)

Table of Contents

1. Materials

Analytical reagents were purchased from Guangdong Guanghua Sci-Tech Co., Ltd. (Shantou, China) and Energy Chemical (Shanghai, China) and used without further purification. The water involved in the experiment is self-made reverse osmosis water in the lab.

2. Instruments and methods

Single crystal X-ray diffraction (SC-XRD) tests were performed on Rigaku XtaLab Pro MM007HF DW X diffractometer at ambient temperature or 250 K.

Powder X-ray diffraction (PXRD) data were collected on Rigaku MiniFlex600 diffractometer using Cu K_α radiation. Patterns were scanned over 3-40° (2θ) with a scan speed of 10°/min and a step width of 0.02°, respectively (Environment: 25 °C, 50% humidity). Samples listed in figure 1 were tested under a wet condition (immersed with a little amount of DMF) to maintain the structure of MIL-88B(Mn).

The morphology and size of manganese MOFs were investigated by using ZEISS Gemini 300 field-emission **scanning electron microscope (SEM)** with an acceleration voltage of 4 kV.

Infrared spectra (IR) were measured from 400 cm^{-1} to 4000 cm^{-1} by Nicolet AVATAR 360 in transition mode. Samples were diluted in KBr pellets.

UV-Vis spetra were recorded on a Shimadzu UV-1780 UV-Vis spectrophotometer (Environment: 25 °C, 50% humidity).

Gas-adsorption was performed on a BSD-PM Specific Surface Area & Pore Size Analyzer (BeiShiDe Instrument, Beijing). Before starting the test, the sample was degassed at room temperature for 1 day after three days of solvent exchange with acetonitrile.

Electron Paramagnetic Resonance (EPR) test was conducted on JES-FA300 Electron Spin Resonance Spectrometer at room temperature with a 9063.389 MHz microwave radiation.

Diffuse reflection spectra (Solid state UV-Vis spectra) were recorded on PerkinElmer Lambda 950 spectrophotometer using $BaSO_4$ as a reference. Scans were measured from 800 nm to 250 nm with a scan width of 0.5 nm.

X-ray photoelectron spectroscopy (XPS) test was performed on Thermo Fisher Scientific - K-Alpha X-ray photoelectron spectrometer.

(Above mentioned three tests were carried out from Guangzhou Puchuan Testing Technology Co., Ltd.)

Magnetic susceptibilities of the polycrystalline samples of MIL-101(Mn)-py were measured on a PPMS DynaCool-9 magnetometer (Quantum Design INC).The measurement was conducted at a magnetic field of 5k Oe and a temperature range from 2 K to 300 K.

Thermogravimetric analysis (TGA) was performed on the TA Instruments Q50 thermogravimetric instrument under N_2 flow (40 $mL \cdot min^{-1}$) and heated from room temperature to 700 °C at a rate of 5 °C min^{-1}。

3. Synthetic procedure

3.1 Synthesis of MIL-101(Mn)

The synthesis method was based on the MIL-88B(Mn) recipe reported by Farha's group[1] with modifications.

140 mg of H_2PTA, 14 mL N, N-dimethylformamide (DMF), 2 mL of acetic acid (HOAc) and different amounts of pyridine derivates were added into a 20 mL vial, which was tightly caped after addition. The glass bottle was heated at 60 °C until all starting materials were completely dissolved. After further adding 40 mg manganese acetate tetrahydrate ($Mn(OAc)_2 \cdot 4H_2O$) and 10 mg potassium permanganate ($KMnO_4$), the solution was ultrasonicated until a clear burgundy solution formed. The vial was subsequently heated at 60 °C for 24 h to obtain dark green crystalline solid. The

crystals were filtered, washed with DMF adequately and preserved in DMF for subsequent characterization.

Note 1: If the ligand and metal salt were straightforward mixed with solvent, it was easy to produce unknown white precipitates, which we suspected may be unreacted ligand or the divalent manganese complexes. Follow-up studies found that pre-heating the ligand solution was more conducive to the reaction.

Note 2: $KMnO_4$ is strongly oxidative while DMF is rather reductive. Acetic acid is also reactive to strong oxidant. One needs to be very careful when mixing these reactants. The best method is to add $Mn(OAc)_2 \cdot 4H_2O$ first (ultrasonically dissolved) then slowly add $KMnO_4$.

Note 3: It is worth noting that DMF in which the crystals are stored needs to be changed several times, about once a day. Due to the large cavity of MIL-101, immersion in DMF facilitates the exchange of unreacted ligands and metal ions from the pores. If the solvent is not refreshed, impurities will deposit on the surface of MOF powder, affecting subsequent characterization and performance tests.

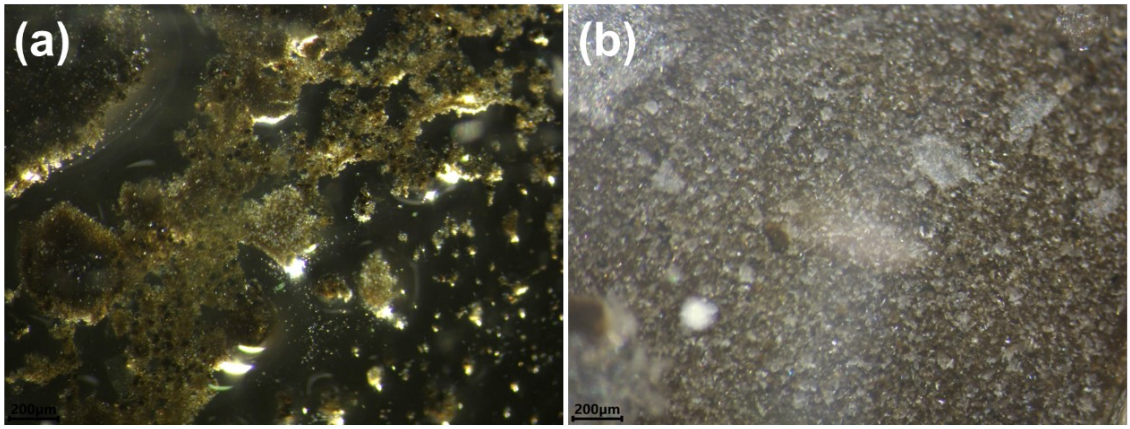

Figure S1 Optical microscope photographs of (a) freshly-prepared MIL-101(Mn) and (b) MIL-101(Mn) soaked in DMF for 1 week without refreshing DMF. White crystalline solid deposited on solid surface of MIL-101(Mn)

Note 4: DMF and pyridine are both available to coordinate with manganese ions. The fresh sample will gradually turn brown if the immersion process takes too long which may be owing to the substitution of pyridine by DMF.

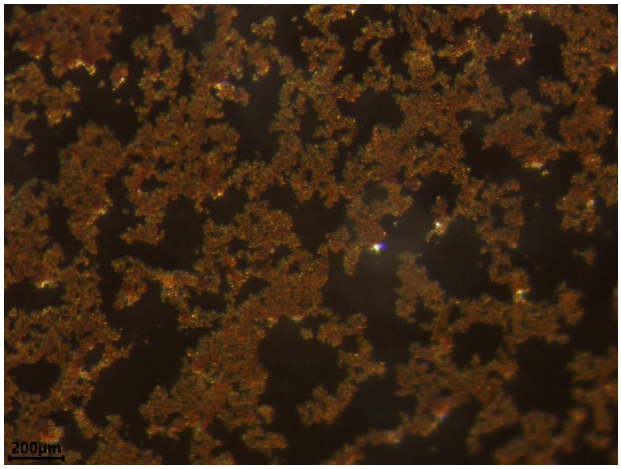

Figure S2 Optical microscope photographs of the brown MIL-101(Mn) crystals after immersing in DMF for 1 month with continuously refreshing DMF.

3.2 Synthesis of single-crystalline MIL-101(Mn)

It is worth noting that it is difficult to obtain pure phase large crystals of MIL-101(Mn) by direct synthesis for single crystal diffraction tests, nevertheless, it is relatively easy to acquire mixed crystals of MIL-101(Mn) and MIL-88B(Mn), as shown in Figure S3.

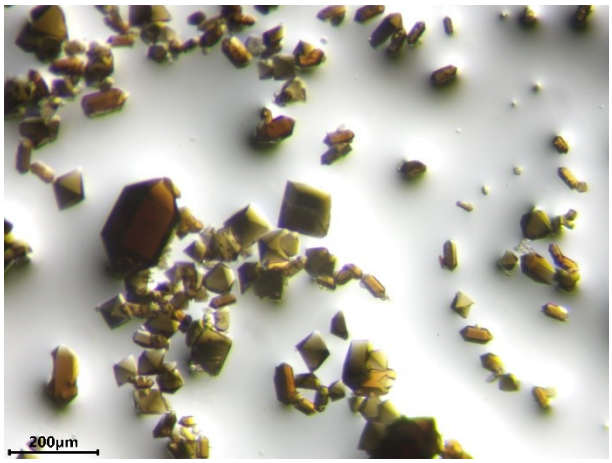

Figure S3 Optical microscope photographs of the mixed crystals. Brown bicapped hexagonal crystals are MIL-88B(Mn), while dark green octahedral crystals are MIL-101(Mn).

Synthetic procedure: 140 mg of H_2PTA, 18 mL N, N-dimethylformamide (DMF), 2 mL of acetic acid (HOAc) and 0.25 ~ 0.3 mL pyridine were added into a 25 mL vial, which was tightly caped after addition. The glass bottle was heated at 60 °C until all starting materials were completely dissolved. After further adding 40 mg $Mn(OAc)_2 \cdot 4H_2O$ and 20 mg $KMnO_4$, the solution was ultrasonicated until a clear burgundy solution formed. The vial was subsequently heated at 60 °C for 24 h to obtain above crystals.

3.3 Synthesis of MIL-101(Mn) at different temperature

The synthetic recipe is similar to the method mentioned in section 3.1, except the synthetic temperature is varied from 50 to 80 °C. At 50 °C, it appeared to be homogenous, indicating the reaction was incomplete. Above 60 °C, the solution became colorless with little or no solid products, which means the over-reduction of manganese.

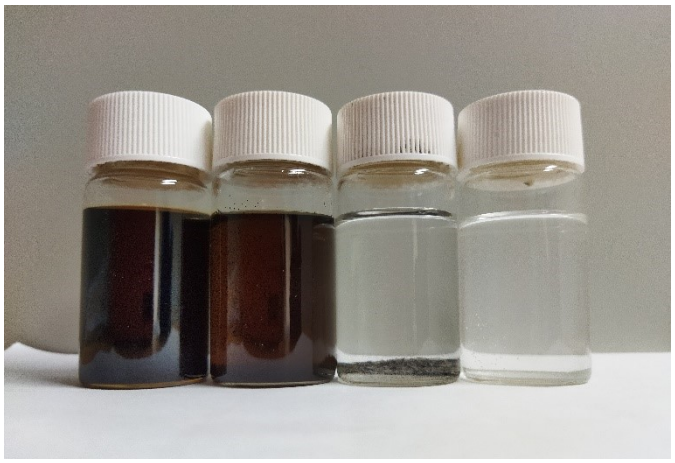

Figure S4 Photograph of MIL-101(Mn) synthesized in different temperature. From left to right: 50, 60, 70, 80 °C.

3.4 Synthesis of MnPTA with different addition of benzoic acid

The synthetic recipe is similar to the method mentioned in section 3.1, except the acetic acid was switch to benzoic acid and no pyridine is added. At higher concentration of benzoic acid (≥320 mg), the MIL-88B phase started to appear. However, no MIL-101 product was obtained during changing the addition of benzoic acid, which indicates the reported method was not applicable in manganese series.

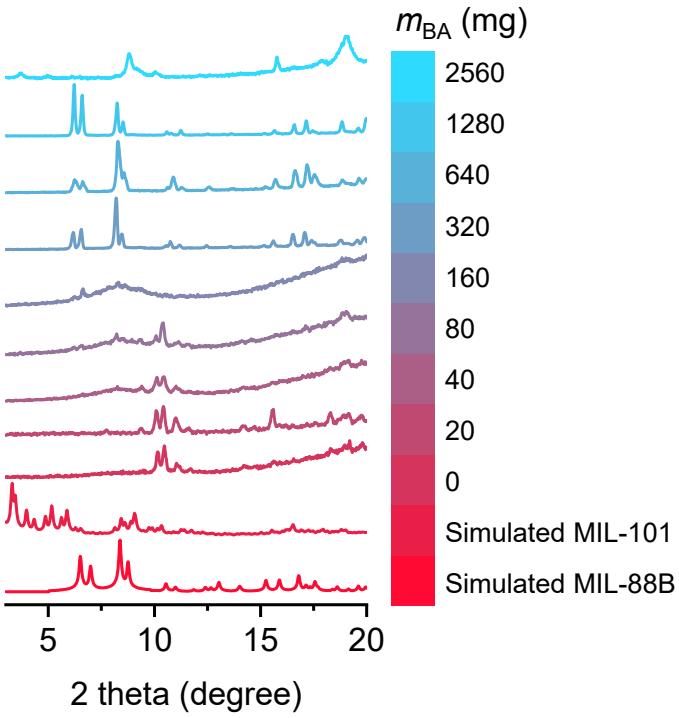

Figure S5 PXRD patterns of synthesized MnPTA MOFs induced by different addition of benzoic acid.

3.5 Synthesis of MIL-88B(Mn) with different addition of 2,6-dimethylpyridine

The synthetic recipe is similar to the method mentioned in section 3.1, except the pyridine was switch to 2,6-dimethylpyridine. No MIL-101(Mn) product was obtained during changing the addition of 2,6-dimethylpyridine, which indicates the failure of phase selection effect of 2,6-dimethylpyridine.

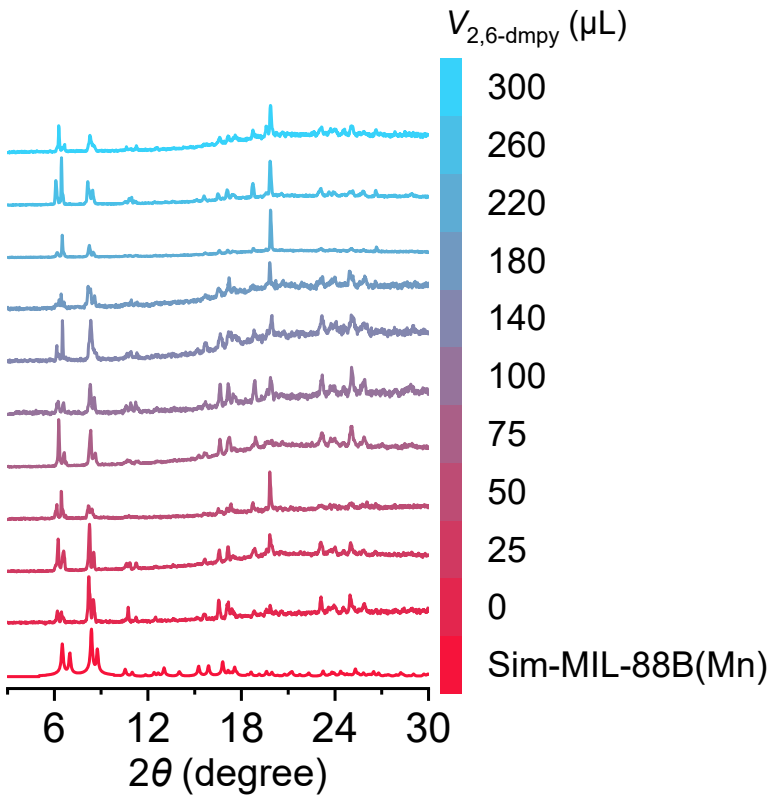

Figure S6 PXRD patterns of synthesized MIL-88B(Mn) with different addition of 2,6-dmpy.

4. Single crystal X-ray crystallography

Single crystals of MIL-101(Mn) was transferred to a microscope slide along with a little mother liquor. A small piece of crystal (about 0.1×0.15×0.2 mm^3) was picked and washed completely in vacuum grease, then mounted using a Dual-Thickness MicroLoop™ (**MiTeGen, Ithaca, New York, USA**).

Data collection was performed on Rigaku Oxford XtaLAB Pro diffractometer equipped with micro focus sealed X-ray tube (Cu K_α radiation, λ = 1.54178 Å) and PILATUS 200 K detector at 250 K. Data reduction, absorption correction was conducted on CrysAlisPro (Rigaku, V1.171.39.7e, 2015). Absorption correction was based on implanted spherical harmonics in SCALE3 ABSPACK.

The structure was solved by direct method using *SHELXS*[2] program or intrinsic phasing method using *SHELXT*[3] implanted in *Olex2*.[4] Refinement with full matrix least squares techniques on F^2 was performed by using *SHELXL*.[2] Non-hydrogen atoms were refined anisotropically and all hydrogen atoms were generated based on riding mode. Crystallographic data and structure refinement results are given in Table S1. Selected bond lengths and angles are shown in Table S2 and S3. The same data collection and reduction procedure were performed on MIL-88B(Mn)-35dmpy. Data of MIL-88B(Mn)-35dmpy were listed in Table S4 – S6.

4.1 Crystallographic data of MIL-101(Mn)

Table S1 Crystallographic data of MIL-101(Mn)

Complex	MIL-101(Mn)
CCDC No.	2190013
Formula	C458 H296 Mn51 N10 O248
Formula weight	12708.97
Temperature (K)	260
Crystal system	Cubic
Space group	$Fd\bar{3}m$
a/Å	90.5152(12)
V/Å^3	741591(28)
Z	16
D_c /g cm^{-3}	0.455
reflns coll.	134206
unique reflns	26443
R_{int}	0.1109
R_1 [$I > 2\sigma(I)$]	0.1103
wR_2 [$I > 2\sigma(I)$]	0.2986
R_1 (all data)	0.1815
wR_2 (all data)	0.3547
GOF	0.933

Table S2 Selected bond lengths/Å for MIL-101(Mn)

Bond lengths/Å		Bond lengths/Å	
Mn(1)-O(4)	1.805(5)	Mn(7)-O(18)	2.084(5)
Mn(1)-O(10)#1	1.949(5)	Mn(7)-O(3)	2.142(12)
Mn(1)-O(10)	1.949(5)	Mn(2)-O(23)	1.915(3)
Mn(1)-N(1)	2.070(12)	Mn(2)-O(11)	1.951(15)
Mn(1)-O(13)	2.101(5)	Mn(2)-O(21)	2.019(7)
Mn(1)-O(13)#1	2.101(5)	Mn(2)-O(21)#5	2.019(7)
Mn(4)-O(4)	1.978(3)	Mn(2)-O(2)	2.054(5)
Mn(4)-O(25)	2.038(5)	Mn(2)-O(2)#5	2.054(5)
Mn(4)-O(24)	2.056(5)	Mn(5)-O(1)	1.921(3)
Mn(4)-O(22)#1	2.085(5)	Mn(5)-O(8)#3	2.017(5)
Mn(4)-O(5)	2.102(7)	Mn(5)-O(7)	2.039(5)
Mn(4)-O(14)#1	2.135(5)	Mn(5)-N(3)	2.060(13)
Mn(6)-O(12)	1.856(4)	Mn(5)-O(17)	2.088(6)
Mn(6)-O(20)	2.012(9)	Mn(5)-O(19)	2.110(6)
Mn(6)-O(9)	2.048(5)	Mn(3)-O(1)	1.892(6)
Mn(6)-O(9)#2	2.048(5)	Mn(3)-N(2)	1.966(11)
Mn(6)-O(16)	2.100(5)	Mn(3)-O(6)	2.029(6)
Mn(6)-O(16)#2	2.101(5)	Mn(3)-O(6)#3	2.029(6)
Mn(7)-O(12)	2.059(7)	Mn(3)-O(15)#3	2.056(5)
Mn(7)-O(18)#2	2.084(5)	Mn(3)-O(15)	2.056(5)
Mn(7)-O(18)#3	2.084(5)	Mn(1)-O(4)	1.805(5)
Mn(7)-O(18)#4	2.084(5)		

Symmetry transformations used to generate equivalent atoms:

#1 -x+1,-z+1/2,-y+1/2 #2 z+1/2,y,x-1/2 #3 -z+3/4,y,-x+3/4 #4 -x+5/4,y,-z+1/4 #5 x,-z+3/4,-y+3/4

#6 -y+3/4,-x+3/4,z #7 -y+5/4,-x+5/4,z #8 -z+3/4,x,-y+3/4 #9 y,-z+3/4,-x+3/4 #10 y,x,z

Table S3 Selected bond angles/° for MIL-101(Mn)

Bond angles/°		Bond angles/°	
O(4)-Mn(1)-O(10)#1	94.89(15)	O(9)#2-Mn(6)-O(16)#2	86.1(2)
O(4)-Mn(1)-O(10)	94.89(15)	O(16)-Mn(6)-O(16)#2	90.7(3)
O(10)#1-Mn(1)-O(10)	170.2(3)	O(12)-Mn(7)-O(18)#2	93.10(17)
O(4)-Mn(1)-N(1)	180.0(4)	O(12)-Mn(7)-O(18)#3	93.10(17)
O(10)#1-Mn(1)-N(1)	85.11(15)	O(18)#2-Mn(7)-O(18)#3	173.8(3)
O(10)-Mn(1)-N(1)	85.11(15)	O(12)-Mn(7)-O(18)#4	93.10(17)
O(4)-Mn(1)-O(13)	97.01(16)	O(18)#2-Mn(7)-O(18)#4	86.6(3)
O(10)#1-Mn(1)-O(13)	90.2(2)	O(18)#3-Mn(7)-O(18)#4	93.1(3)
O(10)-Mn(1)-O(13)	88.6(2)	O(12)-Mn(7)-O(18)	93.10(17)
N(1)-Mn(1a)-O(13)	82.99(16)	O(18)#2-Mn(7)-O(18)	93.1(3)
O(4)-Mn(1)-O(13)#1	97.02(16)	O(18)#3-Mn(7)-O(18)	86.6(3)
O(10)#1-Mn(1)-O(13)#1	88.6(2)	O(18)#4-Mn(7)-O(18)	173.8(3)
O(10)-Mn(1)-O(13)#1	90.2(2)	O(12)-Mn(7)-O(3)	180.0
N(1)-Mn(1)-O(13)#1	82.98(16)	O(18)#2-Mn(7)-O(3)	86.90(17)
O(13)-Mn(1)-O(13)#1	166.0(3)	O(18)#3-Mn(7)-O(3)	86.90(17)
O(4)-Mn(4)-O(25)	94.99(19)	O(18)#4-Mn(7)-O(3)	86.90(17)
O(4)-Mn(4)-O(24)	93.58(18)	O(18)-Mn(7)-O(3)	86.90(17)
O(25)-Mn(4)-O(24)	171.2(2)	O(23)-Mn(2)-O(11)	178.8(4)
O(4)-Mn(4)-O(22)#1	93.41(19)	O(23)-Mn(2)-O(21)	95.5(2)
O(25)-Mn(4)-O(22)#1	88.6(2)	O(11)-Mn(2)-O(21)	85.3(3)
O(24)-Mn(4)-O(22)#1	93.1(2)	O(23)-Mn(2)-O(21)#5	95.5(2)
O(4)-Mn(4)-O(5)	178.9(2)	O(11)-Mn(2)-O(21)#5	85.3(3)
O(25)-Mn(4)-O(5)	84.8(2)	O(21)-Mn(2)-O(21)#5	85.9(4)

O(24)-Mn(4)-O(5)	86.7(2)	O(23)-Mn(2)-O(2)	94.3(3)
O(22)#1-Mn(4)-O(5)	85.5(2)	O(11)-Mn(2)-O(2)	84.8(3)
O(4)-Mn(4)-O(14)#1	92.72(17)	O(21)-Mn(2)-O(2)	170.1(3)
O(25)-Mn(4)-O(14)#1	91.1(2)	O(21)#5-Mn(2)-O(2)	92.3(3)
O(24)-Mn(4)-O(14)#1	86.3(2)	O(23)-Mn(2)-O(2)#5	94.3(3)
O(22)#1-Mn(4)-O(14)#1	173.9(2)	O(11)-Mn(2)-O(2)#5	84.8(3)
O(5)-Mn(4)-O(14)#1	88.3(2)	O(21)-Mn(2)-O(2)#5	92.3(3)
O(12)-Mn(6)-O(20)	180.0(4)	O(21)#5-Mn(2)-O(2)#5	170.1(3)
O(12)-Mn(6)-O(9)	95.3(2)	O(2)-Mn(2)-O(2)#5	87.7(4)
O(20)-Mn(6)-O(9)	84.7(2)	O(1)-Mn(5)-O(8)#3	92.7(2)
O(12)-Mn(6)-O(9)#2	95.3(2)	O(1)-Mn(5)-O(7)	93.3(2)
O(20)-Mn(6)-O(9)#2	84.7(2)	O(9)-Mn(6)-O(16)	86.1(2)
O(9)-Mn(6)-O(9)#2	95.4(3)	O(9)#2-Mn(6)-O(16)	169.6(2)
O(12)-Mn(6)-O(16)	94.7(2)	O(12)-Mn(6)-O(16)#2	94.7(2)
O(20)-Mn(6)-O(16)	85.3(2)	O(20)-Mn(6)-O(16)#2	85.3(2)
O(8)#3-Mn(5)-O(19)	92.1(3)	N(2)-Mn(3)-O(15)	84.0(5)
O(7)-Mn(5)-O(19)	86.7(2)	O(6)-Mn(3)-O(15)	170.2(3)
N(3)-Mn(5)-O(19)	84.5(5)	O(6)#3-Mn(3)-O(15)	92.4(3)
O(17)-Mn(5)-O(19)	169.0(3)	O(15)#3-Mn(3)-O(15)	85.2(3)
O(1)-Mn(3)-N(2)	177.5(5)	Mn(3)-O(1)-Mn(5)	120.09(14)
O(1)-Mn(3)-O(6)	95.7(2)	Mn(3)-O(1)-Mn(5)#3	120.08(14)
N(2)-Mn(3)-O(6)	86.4(5)	Mn(5)-O(1)-Mn(5)#3	119.8(3)
O(1)-Mn(3)-O(6)#3	95.7(2)	Mn(1)-O(4)-Mn(4)#1	120.40(12)
N(2)-Mn(3)-O(6)#3	82.9(4)	Mn(1)-O(4)-Mn(4)	120.40(12)
O(6)-Mn(3)-O(6)#3	88.4(4)	Mn(4)#1-O(4)-Mn(4)	119.2(2)

O(1)-Mn(3)-O(15)#3	94.0(2)	Mn(6)-O(12)-Mn(6)#4	122.5(4)
N(2)-Mn(3)-O(15)#3	87.4(4)	Mn(6)-O(12)-Mn(7)	118.73(19)
O(6)-Mn(3)-O(15)#3	92.4(3)	Mn(6)#4-O(12)-Mn(7)	118.73(19)
O(6)#3-Mn(3)-O(15)#3	170.2(3)	O(9)-Mn(6)-O(16)#2	169.6(2)
O(1)-Mn(3)-O(15)	94.0(2)	O(1)-Mn(5)-O(19)	95.5(2)
O(1)-Mn(5)-O(17)	95.4(2)	O(8)#3-Mn(5)-O(7)	174.0(2)
O(8)#3-Mn(5)-O(17)	88.8(3)	O(1)-Mn(5)-N(3)	178.6(4)
O(7)-Mn(5)-O(17)	91.3(3)	O(8)#3-Mn(5)-N(3)	86.0(4)
N(3)-Mn(5)-O(17)	84.6(5)	O(7)-Mn(5)-N(3)	88.0(4)

Symmetry transformations used to generate equivalent atoms:

#1 -x+1,-z+1/2,-y+1/2 #2 z+1/2,y,x-1/2 #3 -z+3/4,y,-x+3/4 #4 -x+5/4,y,-z+1/4 #5 x,-z+3/4,-y+3/4

#6 -y+3/4,-x+3/4,z #7 -y+5/4,-x+5/4,z #8 -z+3/4,x,-y+3/4 #9 y,-z+3/4,-x+3/4 #10 y,x,z

4.2 Crystal structure of MIL-101(Mn)

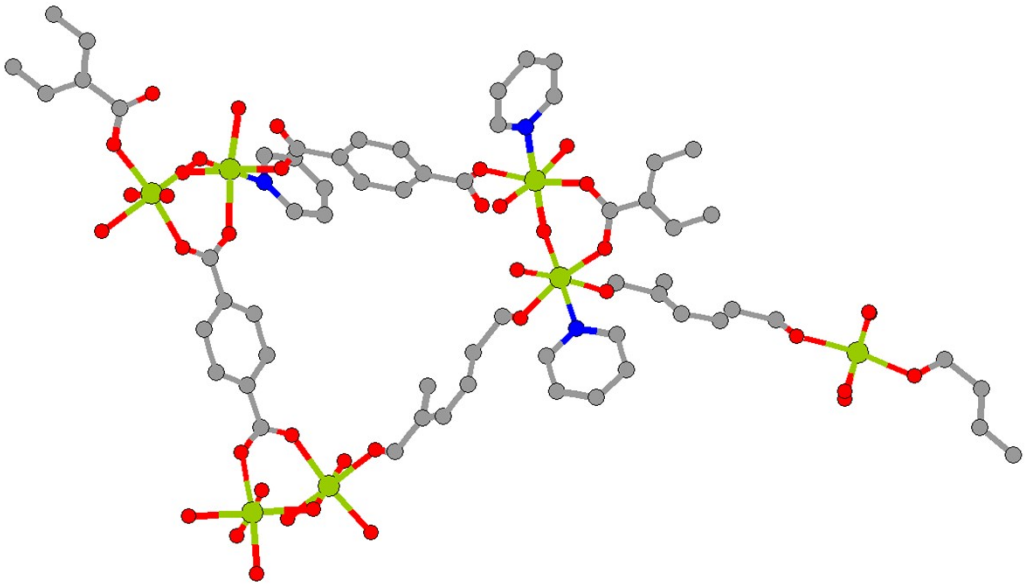

Figure S7 Asymmetic unit of MIL-101(Mn).

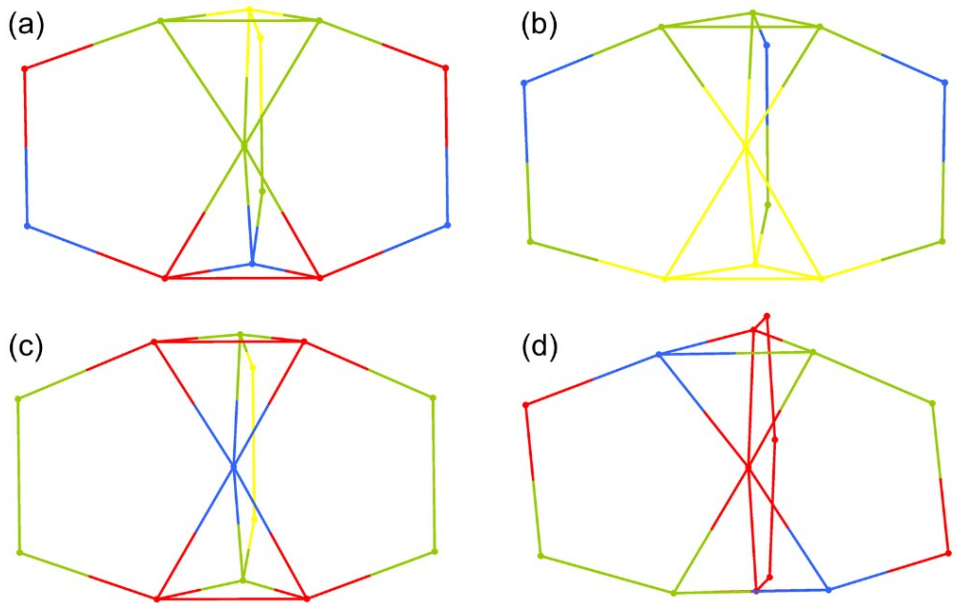

Figure S8 A simple discription of Mn_3^X (X=A, B, C or D) located at the shared-corner of tetrahedrons.

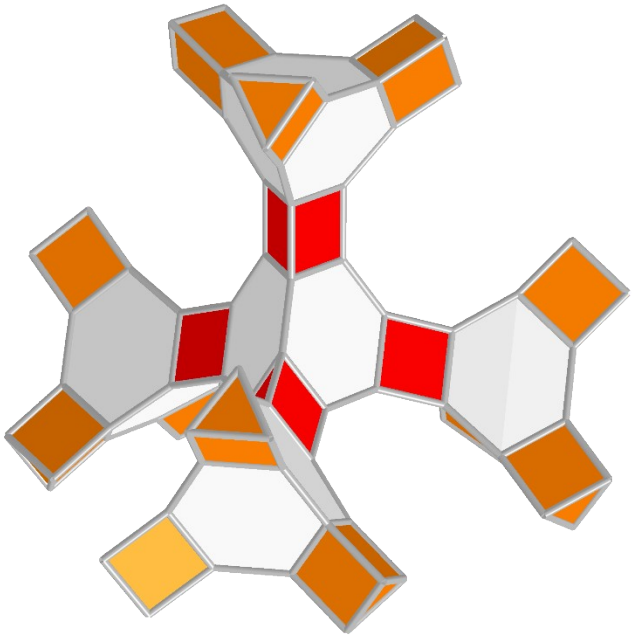

Figure S9 Schematic diagram of a super tetrahedron formed by four Mn_3^B (red) clusters connect with three Mn_3^A (orange) clusters.

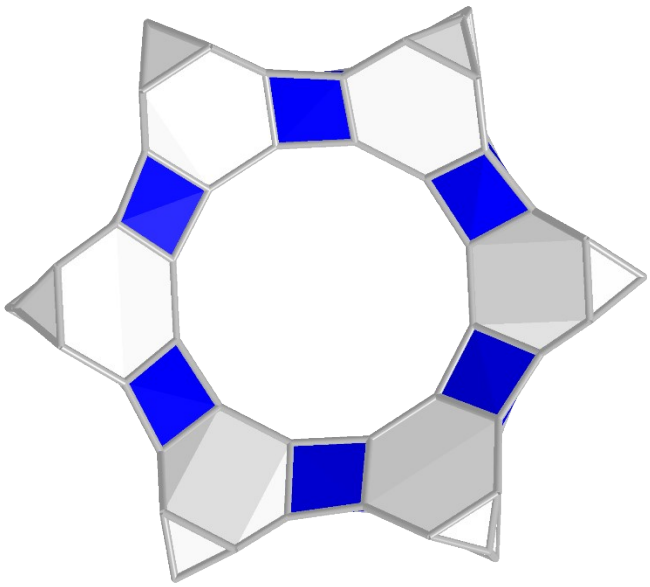

Figure S10 Schematic diagram of the six Mn_3^D clusters forming a hexagonal ring

4.3 Crystallographic data of MIL-88B(Mn)-35dmpy

Table S4 Crystallographic data of MIL-88B(Mn)-35dmpy

Complex	MIL-88B(Mn)-35dmpy
CCDC No.	2190014
Formula	C18 H20 Mn N2 O5.33
Formula weight	404.63
Temperature (K)	293(2) K
Crystal system	Trigonal
Space group	$P\bar{3}1c$
a/Å	15.6573(2)
c/Å	16.4499(2)
V/Å^3	3492.43(10)
Z	6
D_c /g cm^{-3}	1.154
reflns coll.	10659
unique reflns	2228
R_{int}	0.0226
R_1 [$I > 2\sigma(I)$][a]	0.0710
wR_2 [$I > 2\sigma(I)$][b]	0.2311
R_1 (all data)	0.0734
wR_2 (all data)	0.2347
GOF	1.114

Table S5 Selected bond lengths/Å and angles/° for MIL-88B(Mn)-35dmpy

Bond lengths/Å		Bond angles/°	
Mn(1)-O(3)	1.9075(8)	O(3)-Mn(1)-O(2)	93.29(7)
Mn(1)-O(2)	2.070(2)	O(3)-Mn(1)-O(2)#1	93.29(7)
Mn(1)-O(2)#1	2.070(2)	O(2)-Mn(1)-O(2)#1	173.41(13)
Mn(1)-N(1)	2.090(5)	O(3)-Mn(1)-N(1)	180.00(3)
Mn(1)-O(1)#2	2.107(2)	O(2)-Mn(1)-N(1)	86.71(7)
Mn(1)-O(1)#3	2.107(2)	O(2)#1-Mn(1)-N(1)	86.71(7)
		O(3)-Mn(1)-O(1)#2	95.36(7)
		O(2)-Mn(1)-O(1)#2	90.76(10)
		O(2)#1-Mn(1)-O(1)#2	88.63(10)
		N(1)-Mn(1)-O(1)#2	84.64(7)
		O(3)-Mn(1)-O(1)#3	95.36(7)
		O(2)-Mn(1)-O(1)#3	88.63(10)
		O(2)#1-Mn(1)-O(1)#3	90.76(10)
		N(1)-Mn(1)-O(1)#3	84.64(7)
		O(1)#2-Mn(1)-O(1)#3	169.27(14)
		Mn(1)-O(3)-Mn(1)#3	120.0
		Mn(1)-O(3)-Mn(1)#5	120.002(1)
		Mn(1)#3-O(3)-Mn(1)#5	120.0

Symmetry transformations used to generate equivalent atoms:

#1 -y,-x,-z+3/2 #2 x,x-y+1,-z+3/2 #3 -x+y-1,-x,z #4 -x,-y+1,-z+1 #5 -y,x-y+1,z

4.4 Crystal structure of MIL-88B(Mn)-35dmpy

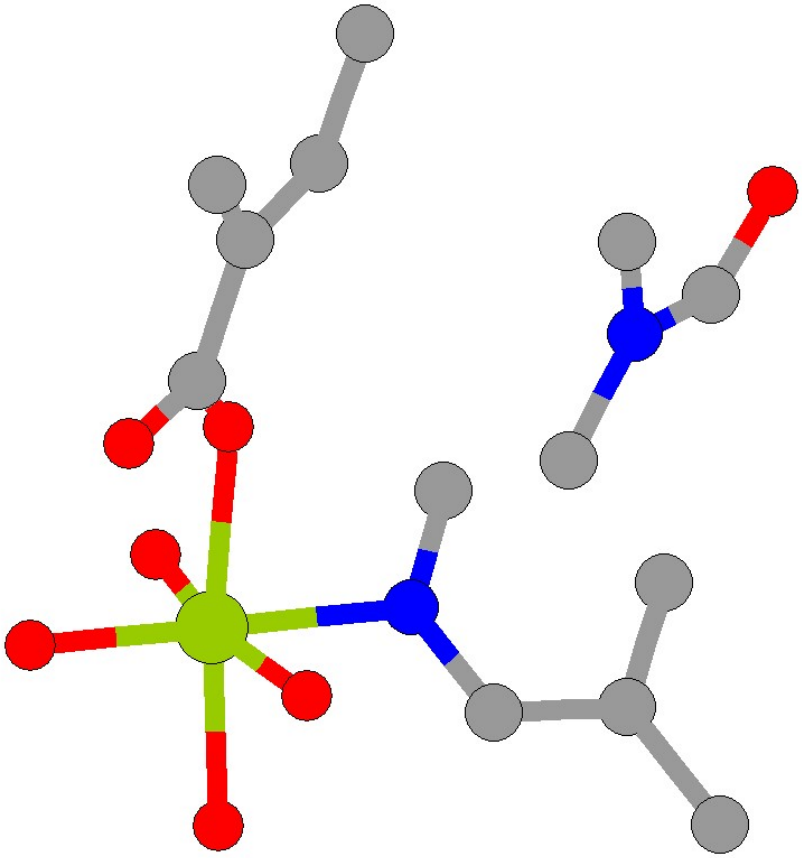

Figure S11 Asymmetric unit of MIL-88B(Mn)-35dmpy

5. Scanning Electron Microscopy (SEM)

MIL-101(Mn)-py was prepared using the method described in section 3.1 using 2 mL pyridine.

In order to avoid crystal damage caused by excessive contact with moisture due to the poor stability of MIL-101(Mn), the sample preparation method for SEM test is as follows:

take 1 mg MIL-101(Mn)-py and ultrasonically disperse in 2 mL DMF, followed by dropping 20 μL on silicon wafer (5 mm * 5 mm). The silicon chip was slightly heated to evaporat solvent with a heating plate. When it is dry, transfer the silicon wafer to the preparation room quickly, stick it on the sample holder with conductive tape, and coating with Pt NPs under vacuum for 3 min. Finally, it was transfered to sample chamber for testing.

It should be noted that MIL-101(Mn)-py shall be regular octahedral particles (~ 740 nm). However, some samples showed concave octahedrons, which may be owing to the irreversible damage of samples during vacuumizing or solvent evaporation process, similar to the reported MIL-100(Mn)[5].

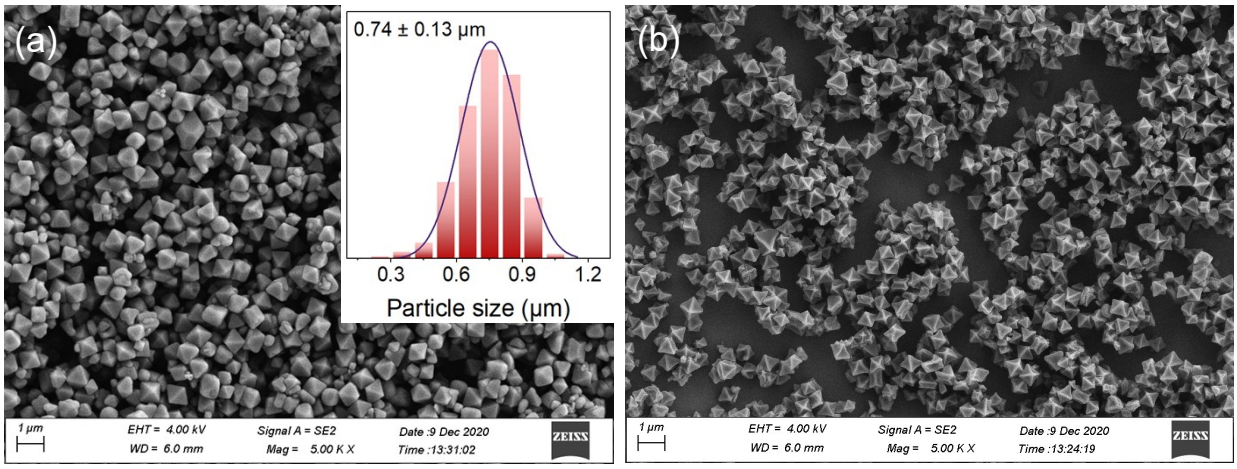

Figure S12 SEM images of (a) regular octahedral and (b) concave octahedral particles of MIL-101(Mn)-py. (inset: statistical distribution of particle sizes)

6. X-Ray Photoelectron Spectra (XPS)

The solid samples were synthesized as follows:

1. MIL-101(Mn)-py: 1.4g H_2PTA + 400 mg $Mn(OAc)_2 \cdot 4H_2O$ + 100 mg $KMnO_4$ + 140 mL DMF + 20 mL HOAc + 20 mL pyridine
2. MIL-101(Mn)-4-Mepy: ~ + 10 mL 4-methylpyridine
3. MIL-101(Mn)-4-tBupy: ~ + 5 mL 4-tertbutylpyridine

The synthesized samples were filtered and washed with DMF (50 mL) and stored in fresh DMF. For liquid samples, pyridine and its derivatives were diluted either with water or ethanol at a ratio of 1:2 (v/v).

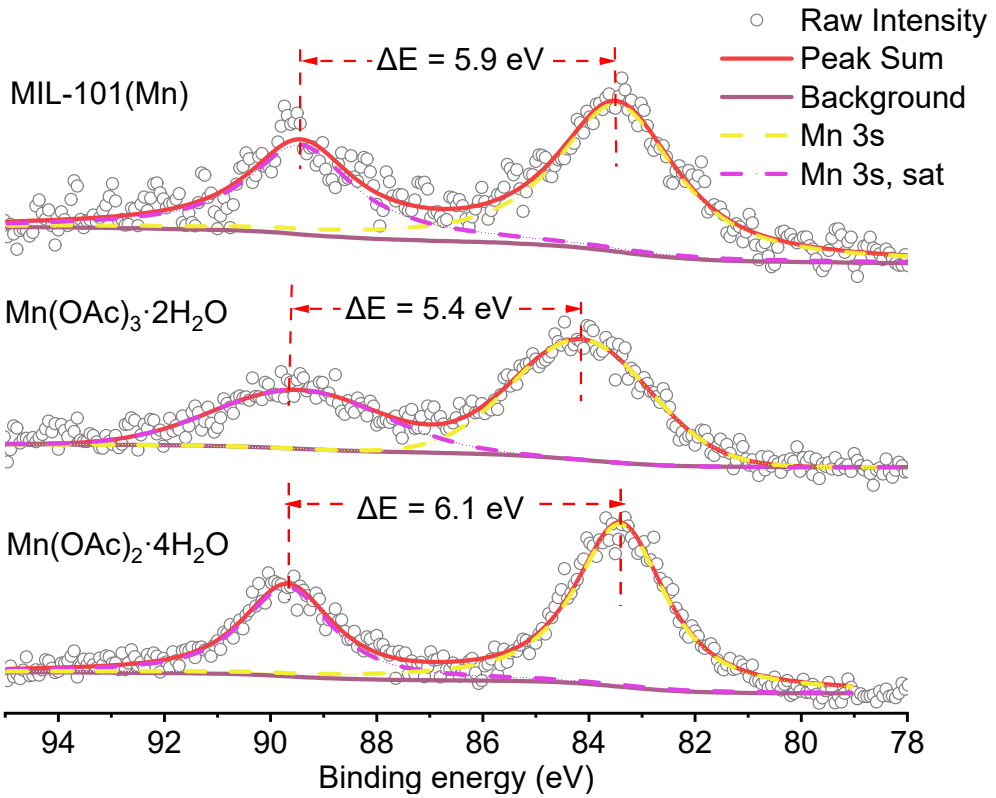

Figure S13 Mn 3s survey of MIL-101(Mn) with referenced Mn(II) and Mn(III) compounds.

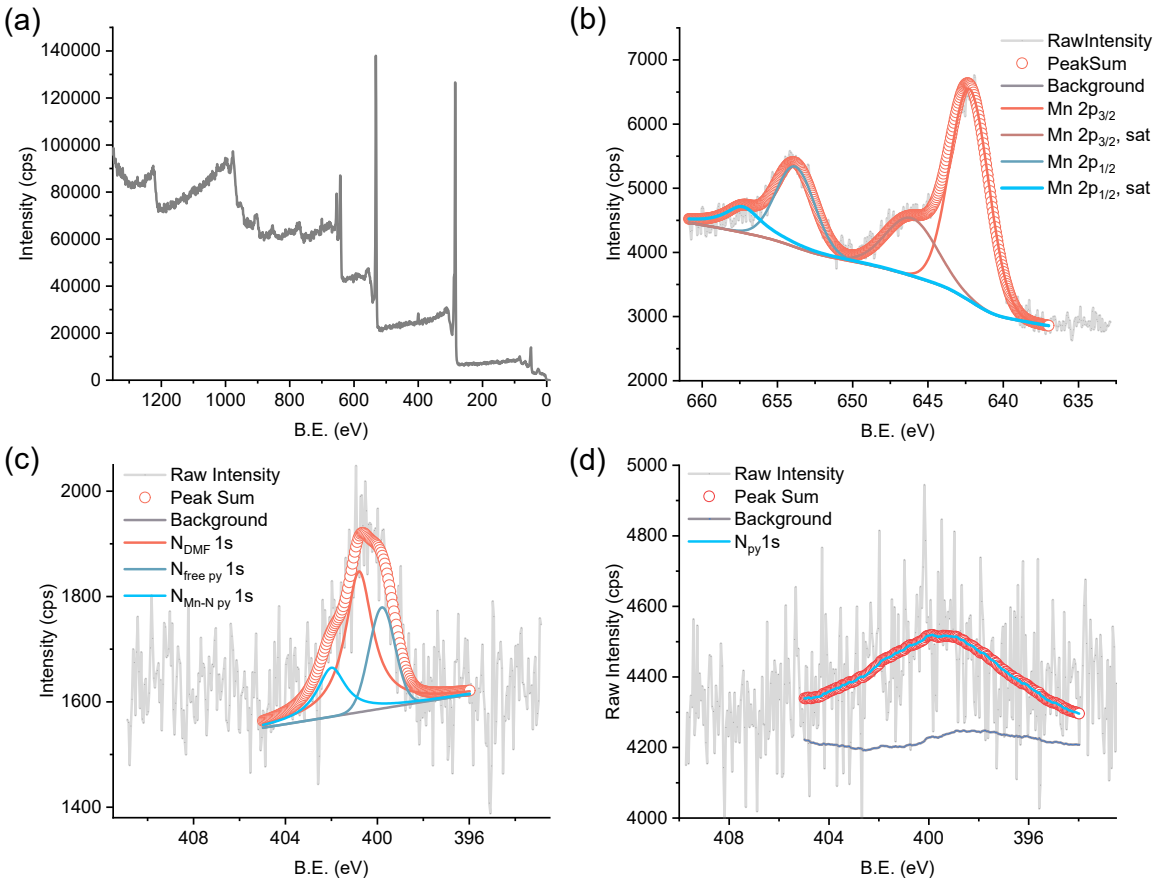

Figure S14 XPS spectra: (a) survey spectrum, (b) Mn 2p, (c) N 1s of MIL-101(Mn)-py, and (d) N 1s of pyridine.

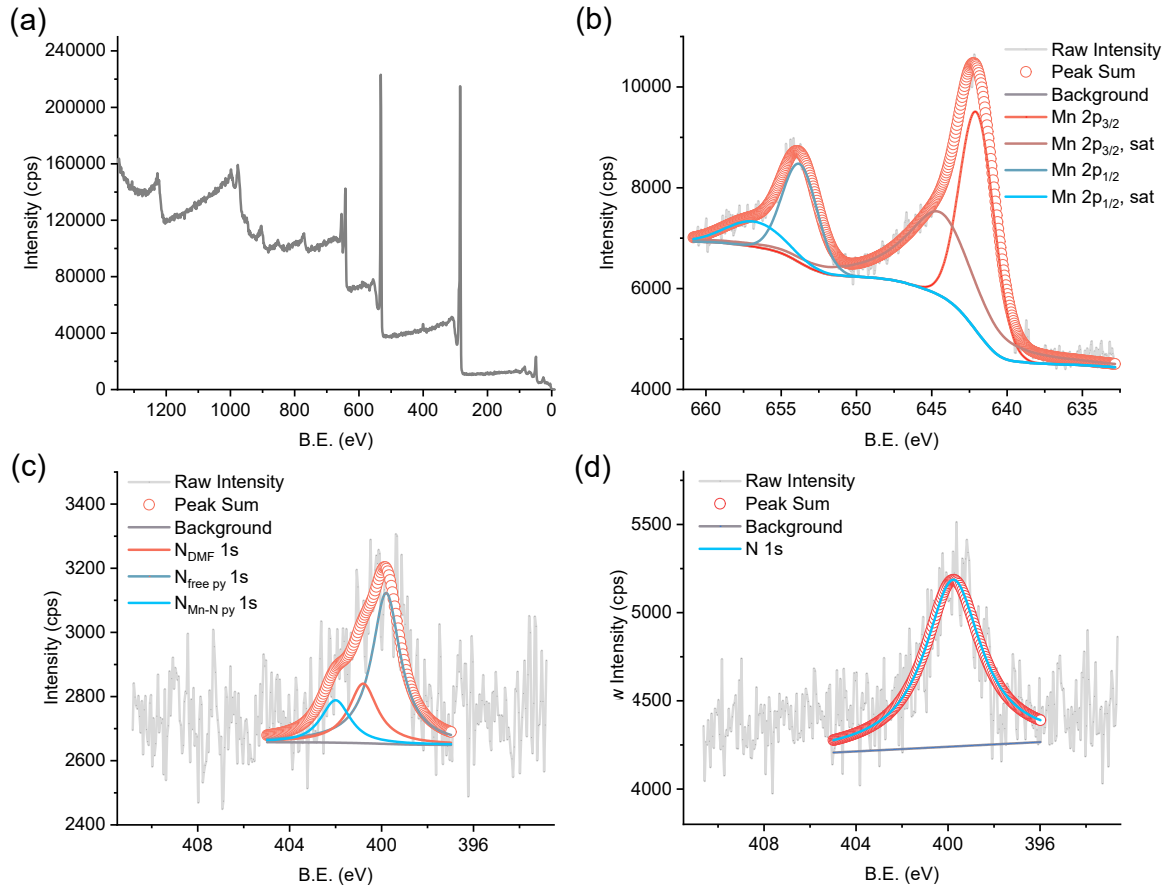

Figure S15 XPS spectra: (a) survey spectrum, (b) Mn 2p, (c) N 1s of MIL-101(Mn)-4-Mepy, and (d) N 1s of 4-methylpyridine.

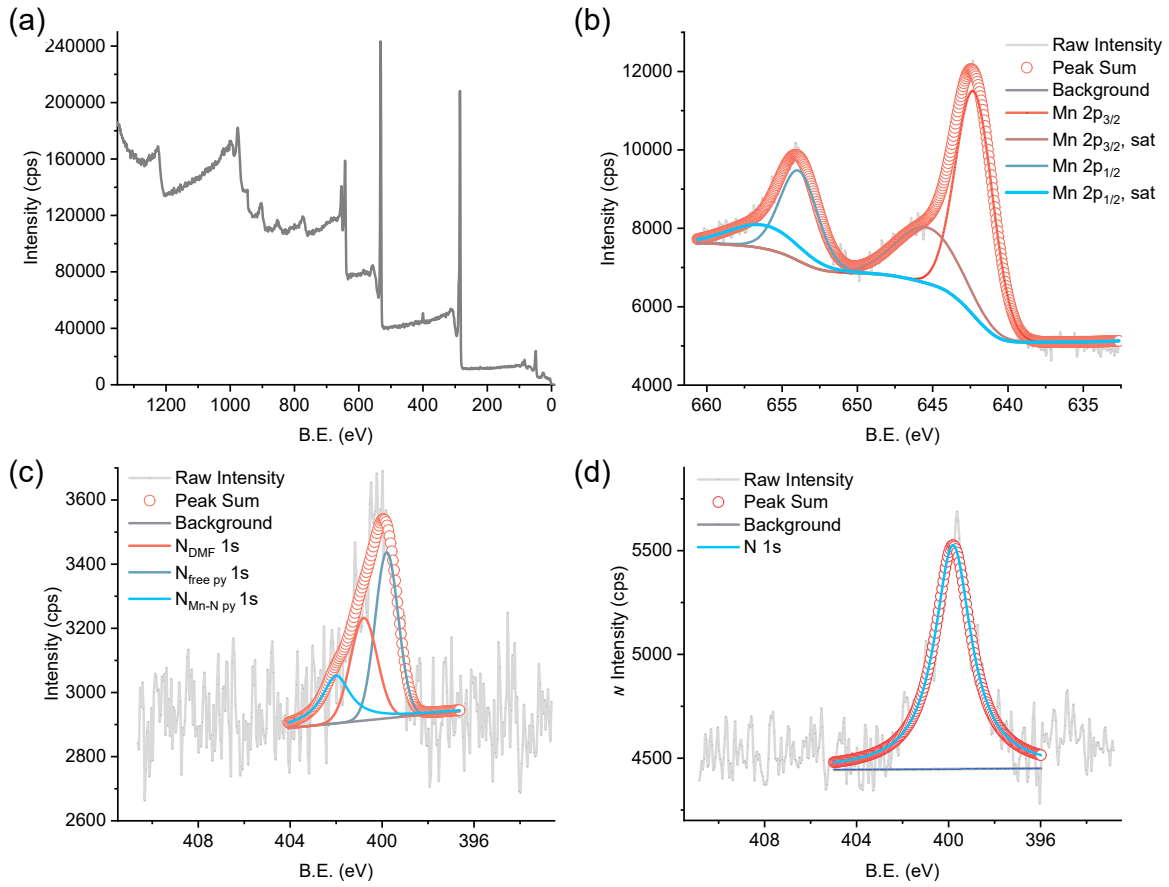

Figure S16 XPS spectra: (a) survey spectrum, (b) Mn 2p, (c) N 1s of MIL-101(Mn)-4-tBupy, and (d) N 1s of 4-tertbutylpyridine.

7. Diffuse reflection spectra

The solid samples were synthesized and handled as mentioned in section 6.

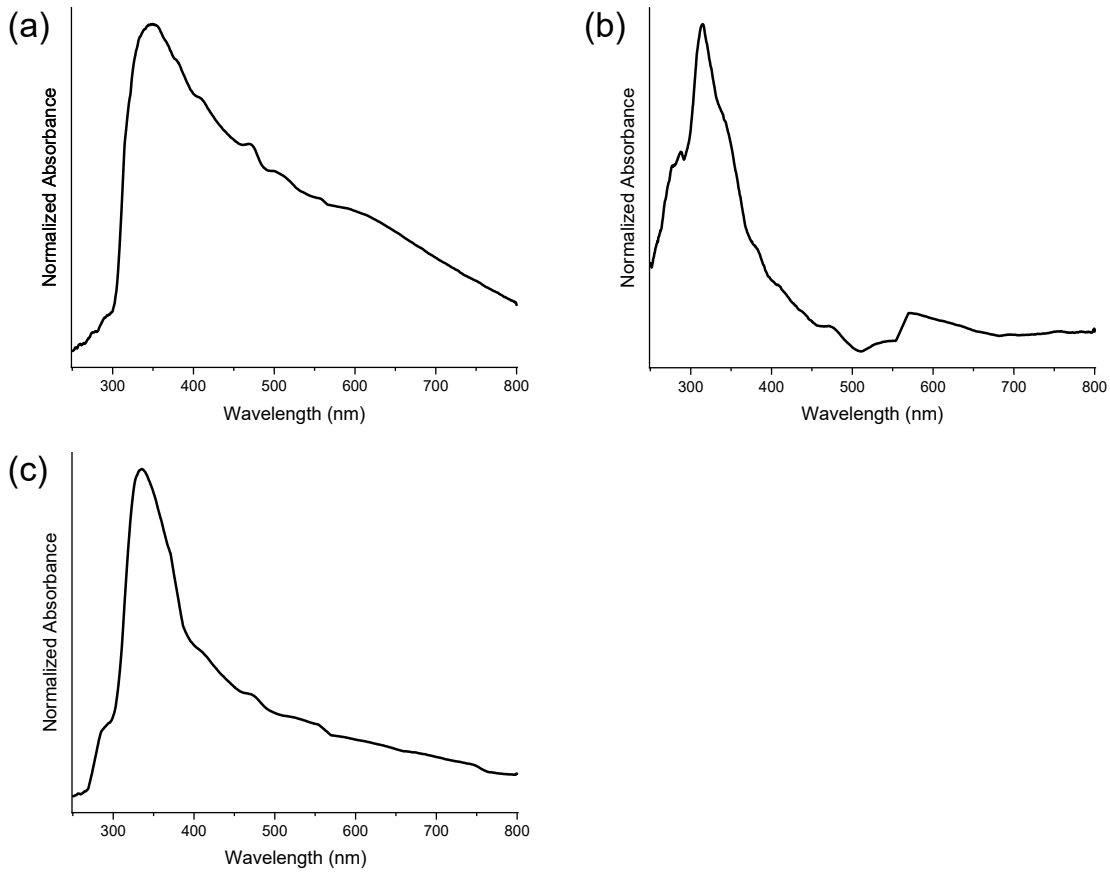

Figure S17 UV spectrum of (a) MIL-101(Mn)-py, (b) MIL-101(Mn)-4-Mepy and (c) MIL-101(Mn)-4-tBupy.

8. Magnetic testing

8.1 Molar magnetization-temperature relationship

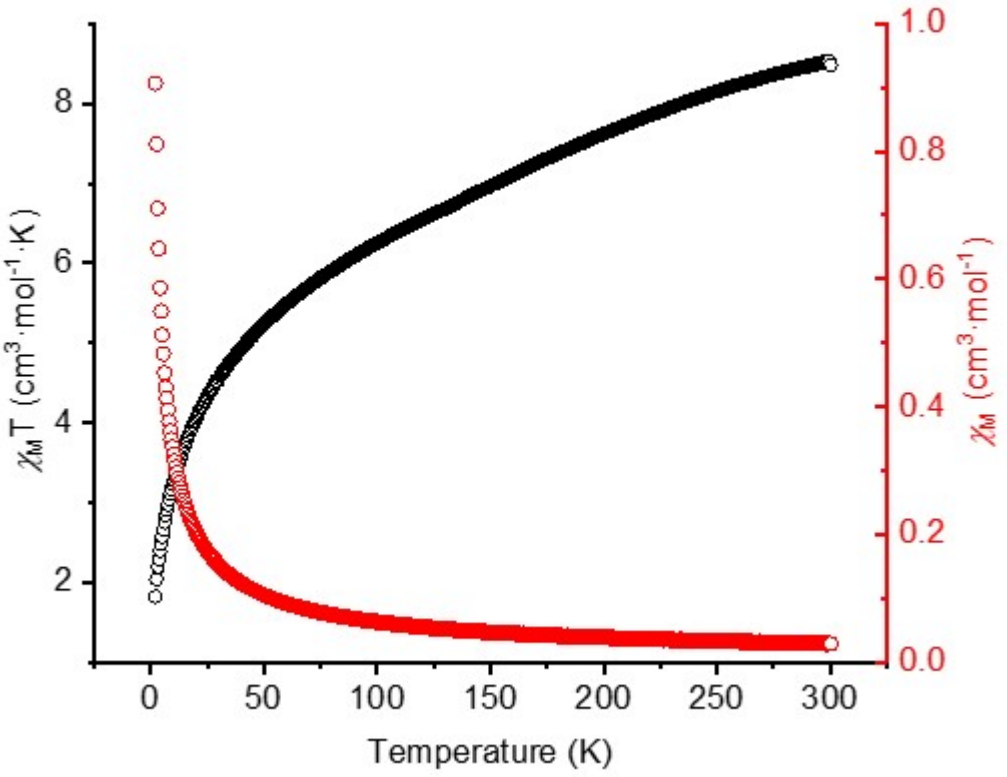

Figure S18 Molar magnetization-temperature curve of MIL-101(Mn)-py.

8.2 Curie-Weiss fitting

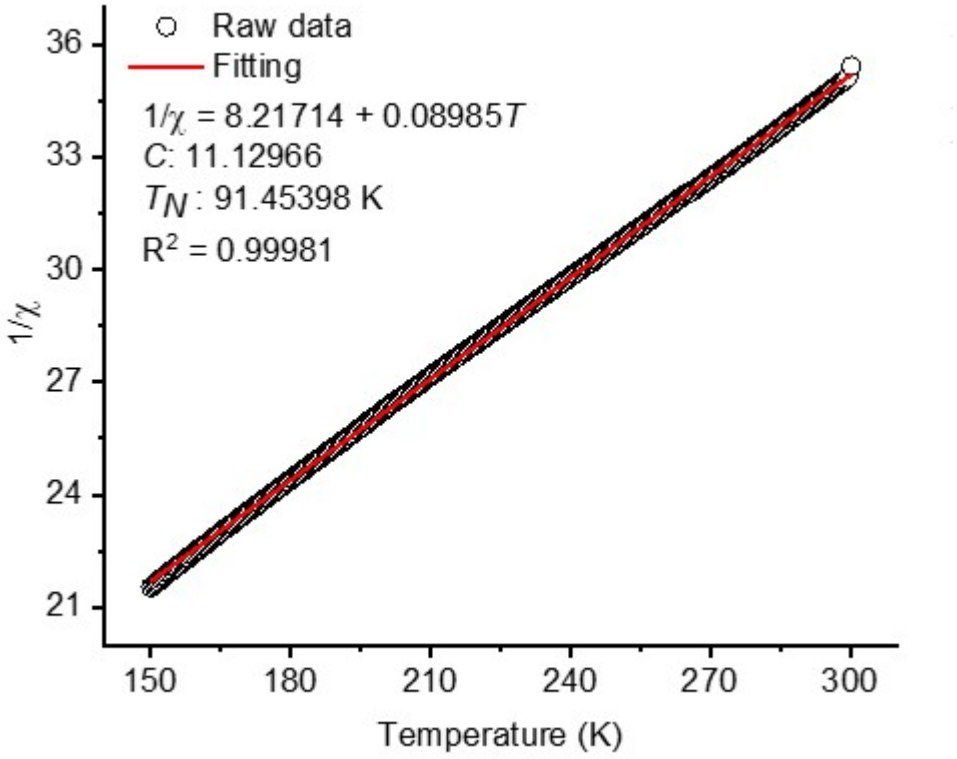

Figure S19 Curie-Weiss fitting curve of MIL-101(Mn)-py.

8.3 Magnetic susceptibilities data and its fitting procedure

Magnetic susceptibilities data of MIL-101(Mn)-py was fitted using *PHI.*[6]

Survey mode was first used to give the possible range of variables, following the previous reported method.[6] The minimum residual interval is taken as the value range of the final optimization, and the appropriate initial value within the range is used to optimize the final result.

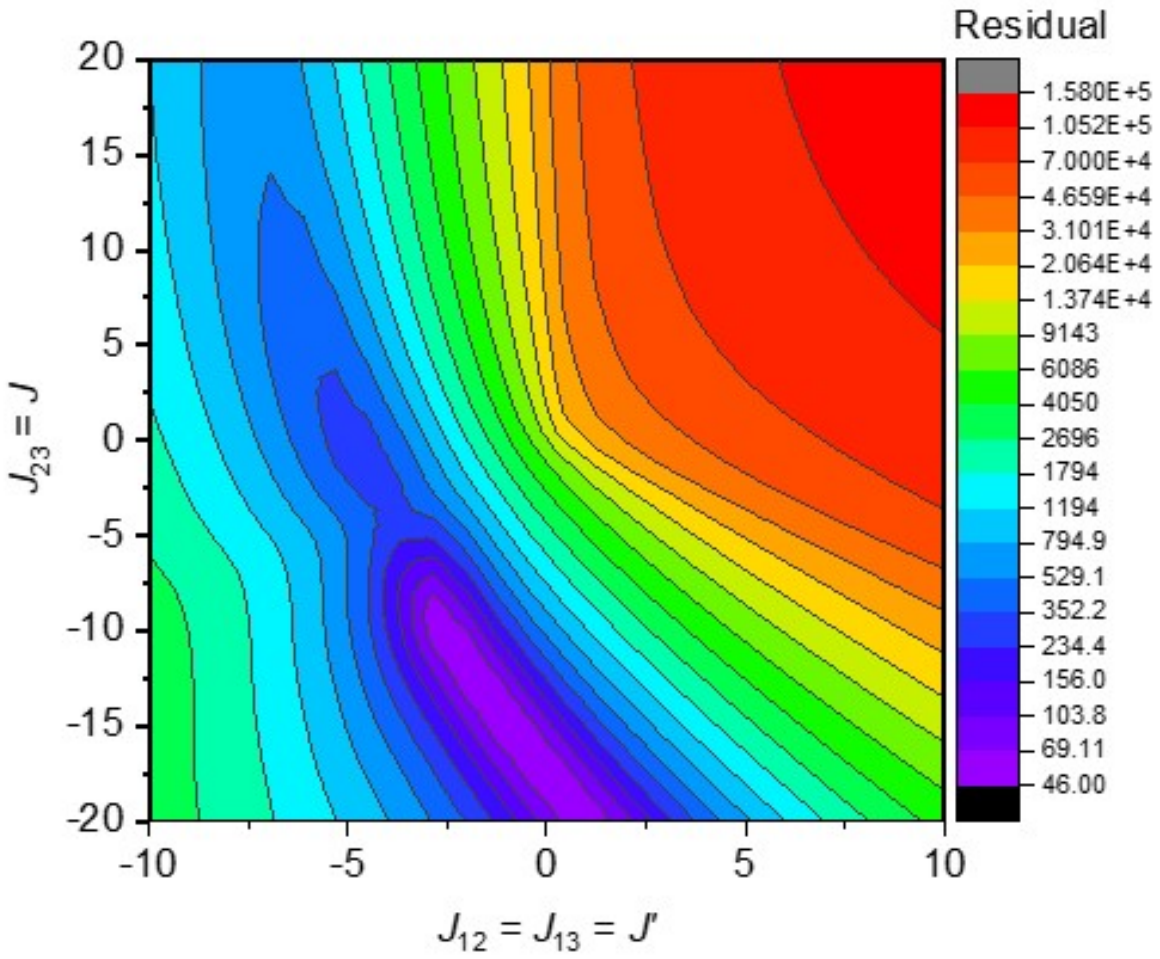

Figure S20 Residual survey for *J* values. Residual$_{min}$ = 46.1316, for *J'* = -2.04082 and *J* = -11.8367

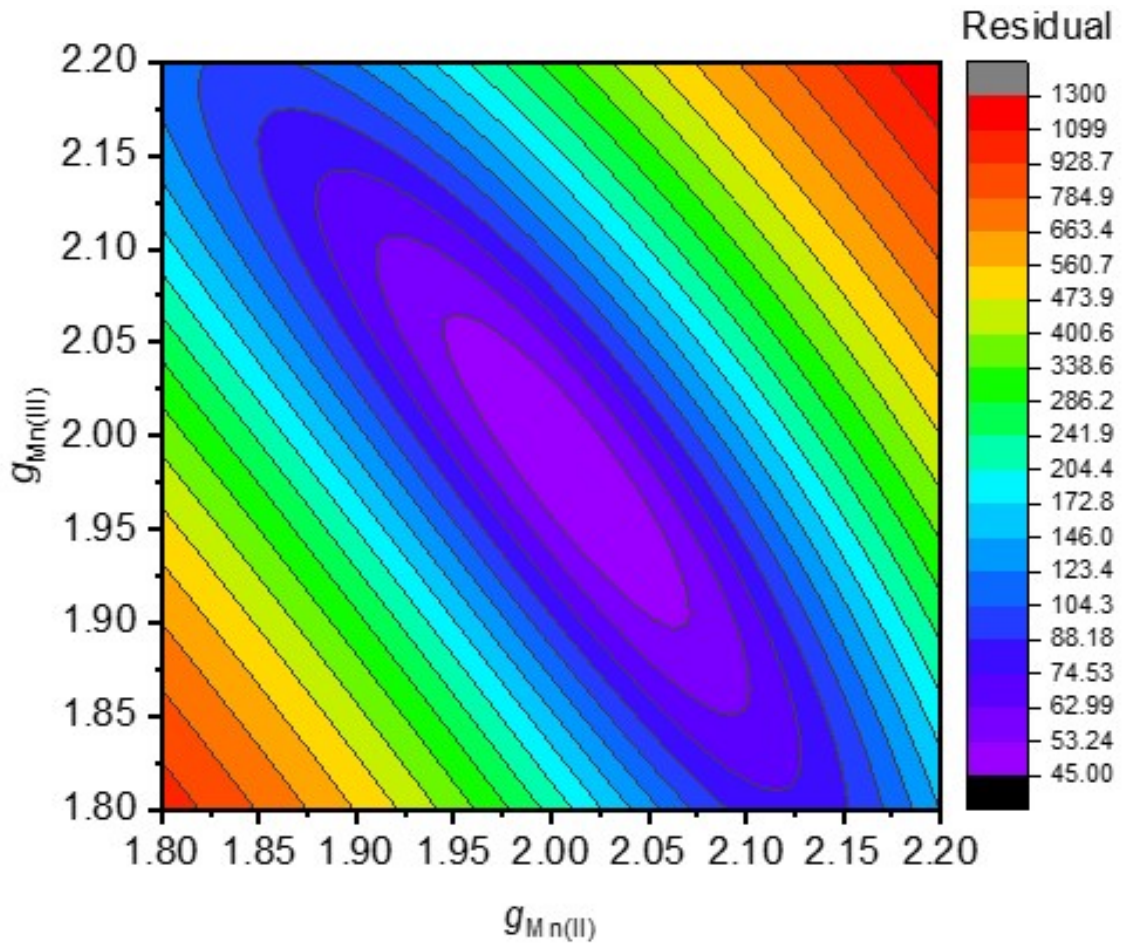

Figure S21 Residual survey for *g* values. $Residual_{min}$ = 45.7783, for $g_{Mn(II)}$= 2.01224 and $g_{Mn(III)}$= 1.97959

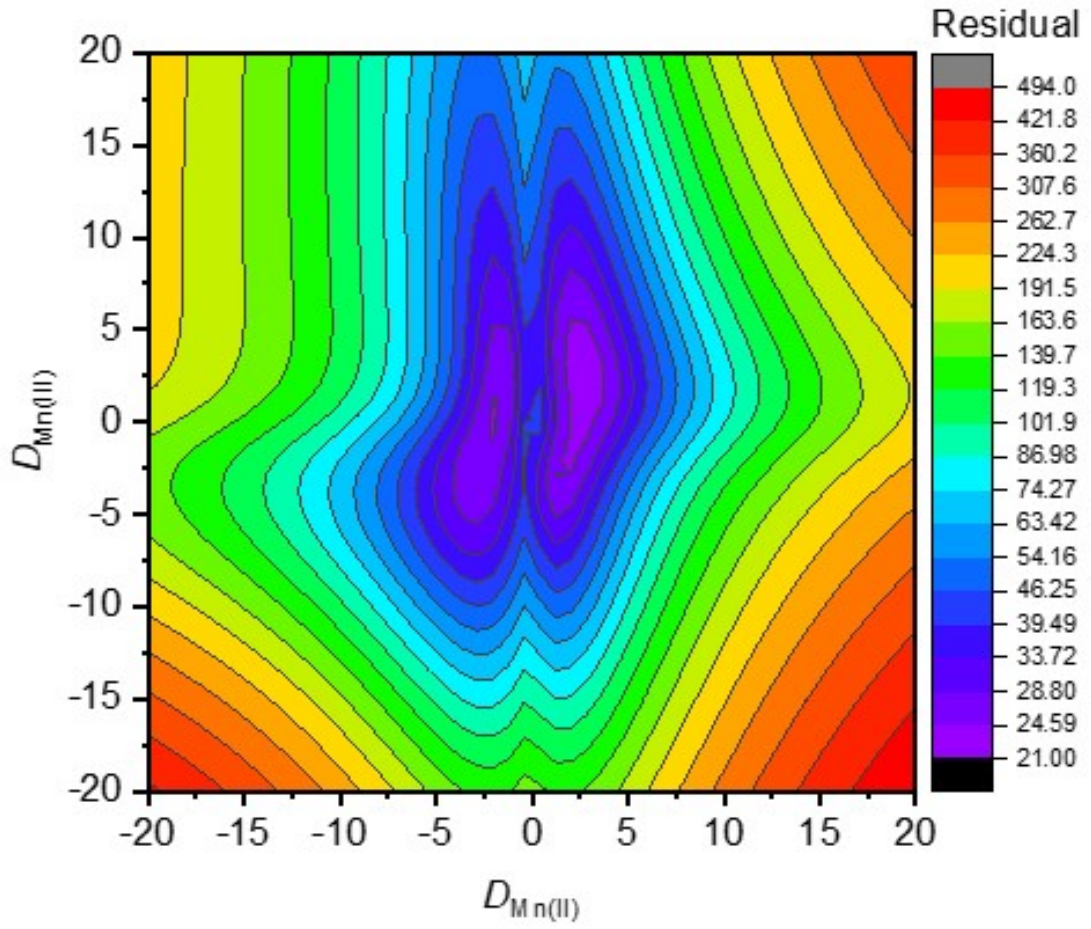

Figure S22 Residual survey for *D* values. Residual$_{min}$ = 21.9715, for $D_{Mn(II)}$= 2.85714 and $D_{Mn(III)}$= 2.04082

9. Infrared spectra (IR)

The solid samples were synthesized and handled as mentioned in section 6.

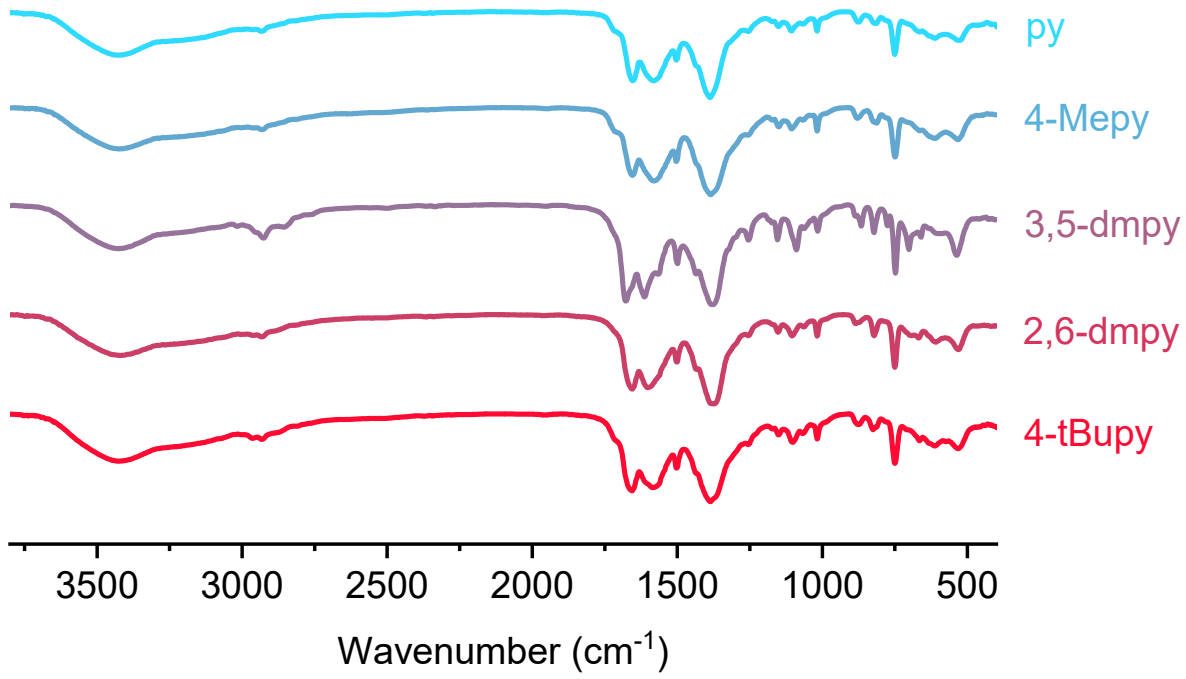

Figure S23 IR spectrum of different MIL-101(Mn) or MIL-88B(Mn) synthesized with various pyridine deriviates.

10. Electron paramagnetic resonance

The solid samples were synthesized and handled as mentioned in section 6.

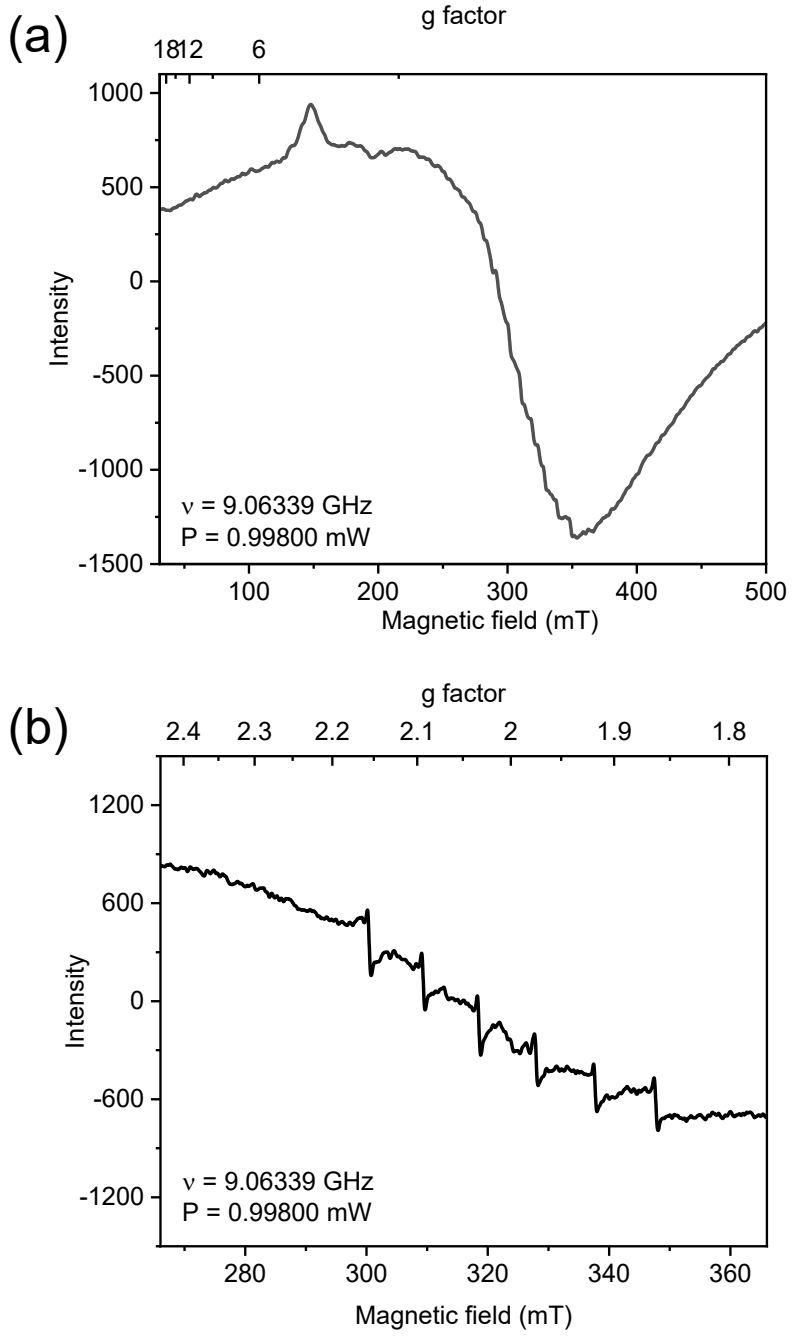

Figure S24 EPR spectra of MIL-101(Mn)-py

11. Theoretical calculation

11.1 Molecular structural optimization

To better understand and obtain the molecular sizes of the several guest, density functional theory (DFT) geometry optimization in the gas phase is performed using the Gaussian 09 program package at the PBE0/6-31g(d,p) level[7–10].

1. Optimized pyridine cartesian coordinates

C	-1.13531300	-0.71780800	0.00001700
C	1.13508200	-0.71815300	0.00004100
C	1.19083300	0.66810000	-0.00000600
C	0.00021200	1.37630500	-0.00002600
C	-1.19064500	0.66840800	0.00001000
H	-2.05060100	-1.30239100	0.00005100
H	2.05024400	-1.30294300	0.00005300
H	2.14724200	1.17562000	0.00001300
H	0.00032000	2.45981500	0.00000100
H	-2.14687200	1.17627300	0.00003500
N	-0.00019300	-1.40964100	-0.00005300

2. Optimized 4-methylpyridine cartesian coordinates

C	1.21393000	-1.13060900	0.00243600
C	1.21446200	1.13029900	0.00241400
C	-0.17043300	1.18349900	-0.00799000
C	-0.90024400	0.00032800	-0.01104900
C	-0.17080900	-1.18329200	-0.00800100
H	1.79203300	-2.05044700	0.00300400
H	1.79285000	2.04996700	0.00300800
H	-0.67484100	2.14317200	-0.01682100
H	-0.67554400	-2.14280900	-0.01686700
N	1.91296800	-0.00022300	0.00769200

C	-2.39646300	0.00019200	0.00694900
H	-2.80049600	-0.87638300	-0.50100600
H	-2.76688500	-0.01849500	1.03594700
H	-2.80055400	0.89405200	-0.46965400

3. Optimized 4-tertbutylpyridine cartesian coordinates

C	2.18775300	-1.12647800	0.00001400
C	2.21399900	1.12871000	-0.00002600
C	0.82703700	1.19805200	-0.00004900
C	0.07740700	0.02785200	-0.00004700
C	0.80483600	-1.16184700	-0.00004200
N	2.90292400	-0.00445400	0.00002500
H	2.75334500	-2.05401300	0.00008000
H	2.79848900	2.04474700	-0.00000600
H	0.30419300	-2.12254800	-0.00009400
H	0.35237400	2.16990700	-0.00007300
C	-1.44527800	0.00738500	-0.00001000
C	-1.93827800	-0.72907900	-1.25124500
H	-1.57399300	-1.75701000	-1.28535500
H	-3.03054000	-0.76032800	-1.26156400
H	-1.60362300	-0.22408400	-2.15980600
C	-1.93814000	-0.72924500	1.25117700
H	-1.60294300	-0.22468600	2.15978300
H	-3.03041000	-0.76004000	1.26187800
H	-1.57428000	-1.75734900	1.28485800
C	-2.03925400	1.41299000	0.00014900
H	-1.74208400	1.97901600	0.88567700
H	-1.74225000	1.97916600	-0.88533400
H	-3.12923700	1.34836200	0.00025600

4. Optimized 3,5-dimethylpyridine cartesian coordinates

C	1.13432500	1.12598500	0.00018000
C	-1.13433000	1.12599300	-0.00020200
C	-1.20558500	-0.26400300	-0.00003400
C	-0.00000400	-0.95298700	0.00019400
C	1.20556700	-0.26404000	0.00020000
N	0.00001200	1.81377000	-0.00000800
H	-0.00001400	-2.03972800	0.00046000
H	2.05108400	1.71101000	0.00043600
H	-2.05107100	1.71104400	-0.00033500
C	-2.52278300	-0.97563200	-0.00001100
H	-2.62766300	-1.61596100	-0.87924000
H	-2.62839600	-1.61461300	0.88011600
H	-3.35239500	-0.26788500	-0.00090400
C	2.52279100	-0.97562300	-0.00019000
H	2.62547600	-1.62071900	0.87577900
H	2.63062900	-1.60981600	-0.88353500
H	3.35238200	-0.26788400	0.00646300

5. Optimized 2,6-dimethylpyridine cartesian coordinates

C	-1.15042300	-0.27063900	0.00000300
C	1.15037800	-0.27069800	0.00006900
C	1.19194800	1.12047200	0.00001600
C	0.00004000	1.82243600	-0.00002200
C	-1.19192000	1.12048400	-0.00001400
H	2.14416100	1.63720600	0.00002000
H	-2.14408500	1.63730600	-0.00000700
N	-0.00001300	-0.94424800	-0.00001600
H	0.00001800	2.90645700	-0.00000200
C	2.41099500	-1.08149000	-0.00001600
H	3.02019400	-0.86119800	-0.88016600

H	3.02084400	-0.86042500	0.87948600
H	2.16407700	-2.14129600	0.00051300
C	-2.41101400	-1.08146700	0.00000800
H	-3.02064400	-0.86069500	0.87973700
H	-3.02046000	-0.86095000	-0.87991300
H	-2.16403600	-2.14125800	0.00017900

11.2 Molecular size calculation

To calculate the size of the molecules, knowing the radius and direction is essential. Van der Waals radii are generally used to calculate the molecular size. Mantina et al. obtained a set of radii data including all the elements of the main group by using computational methods.[11] After having the van der Waals radii and the three vertical directions to use for molecular size calculation, as well as considering the rotation of molecules, the size of the molecules can be described by three maximum distance projected by all atoms on the given principal axes of inertia. By inputing the coordinates of the atoms in the molecule and the radius used, the size of the molecule can be easily obtained from a online tool developed by Jerkwin.[12]

11.3 Description of critical size of the coordinated molecule

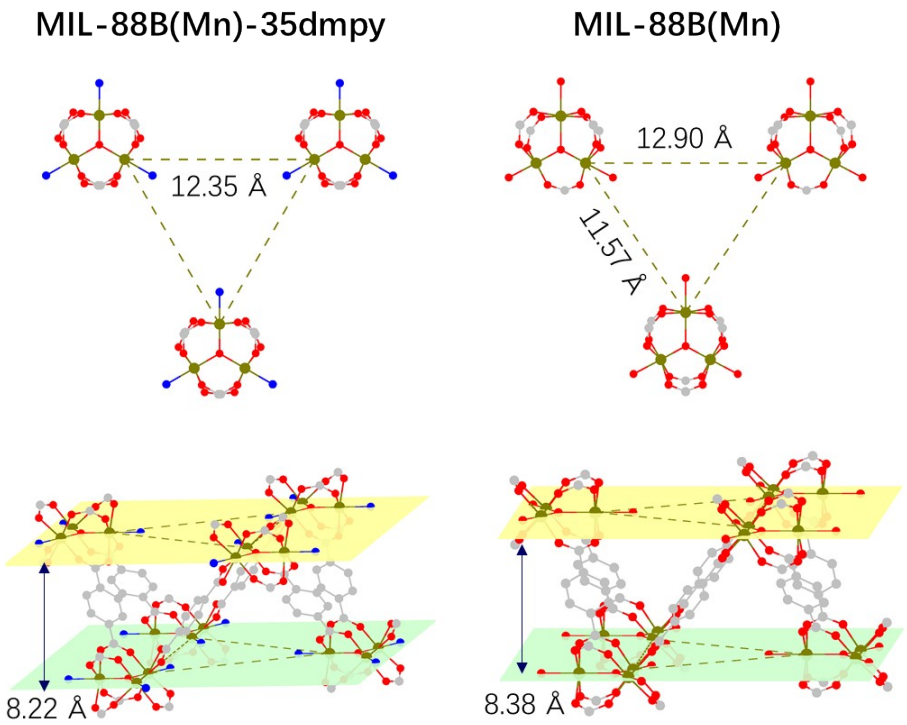

Figure S25 Geometry factors for the description of critical size of the coordinated molecule in MIL-88B(Mn) and MIL-88B(Mn)-35dmpy

We consider the case of MIL-88B(Mn)-35dmpy and previously reported MIL-88B(Mn). For the triangular window in the c-axis direction, the critical distances of Mn to the centero of the triangle are geometrically calculated as 7.13 Å and 6.93 Å. Since the bond length of the Mn-N bond is about 2.10 Å and the van der Waals radius of the N atom is 1.53 Å, the critical dimensions of the ligand molecule axially are 6.56 Å and 6.36 Å, respectively. Next, we consider the layer distances of the two adjacent layers. For MIL-88B(Mn)-35dmpy, the layer distance is 8.22 Å, which is slightly smaller than that of 8.38 Å in MIL-88B(Mn).

For pyridine, the axial length (6.53 Å) is slightly larger than the critical size of MIL-88B(Mn), but such size effect is not as significant as that of 4-methylpyridine (7.54 Å) and 4-tertbutylpyridine (8.66 Å). Nevertheless, for 3,5-dimethylpyridine, although its

axial length (6.51 Å) is greater than the critical size of MIL-88B(Mn), the perfectly fitting of the layer spacing makes it generate another phase of MIL-88B.

11.4 Theoretical surface area

Theoretical surface area was calculated using *iRASPA*.[13] Pyridine molecules are coordinatedly disordered within the MOF structure. In order to give a possible range of the value, surface areas were calculated based on a fully coordinated model and a non-coordinated model. N_2 was used as probing molecule.

For fully coordinated model, it was calculated as 3049.09034 m^2/g, while 3579.01449 m^2/g was calculated by using the non-coordinated model.

12. Stability Test

The solid samples were synthesized and handled as mentioned in section 6.

12.1 Air stability

The air stability of MIL-101(Mn) was tested via the method describe as follows. As-synthesized MIL-101(Mn) was filtered and fully washed with DMF, and transferred onto weighing papers. After that the samples' crystallinities were tested via XRD every once in a while.

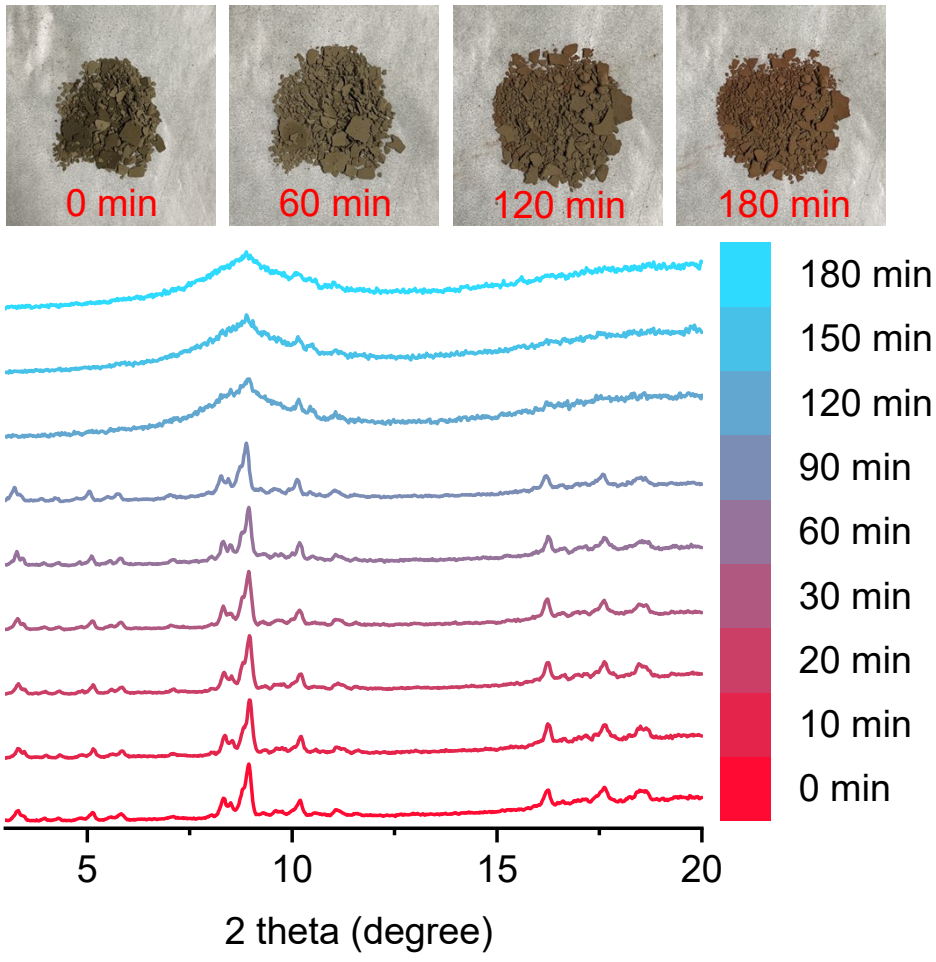

Figure S26 Air stability of MIL-101(Mn)-py. The pictures were taken every 1 hour.

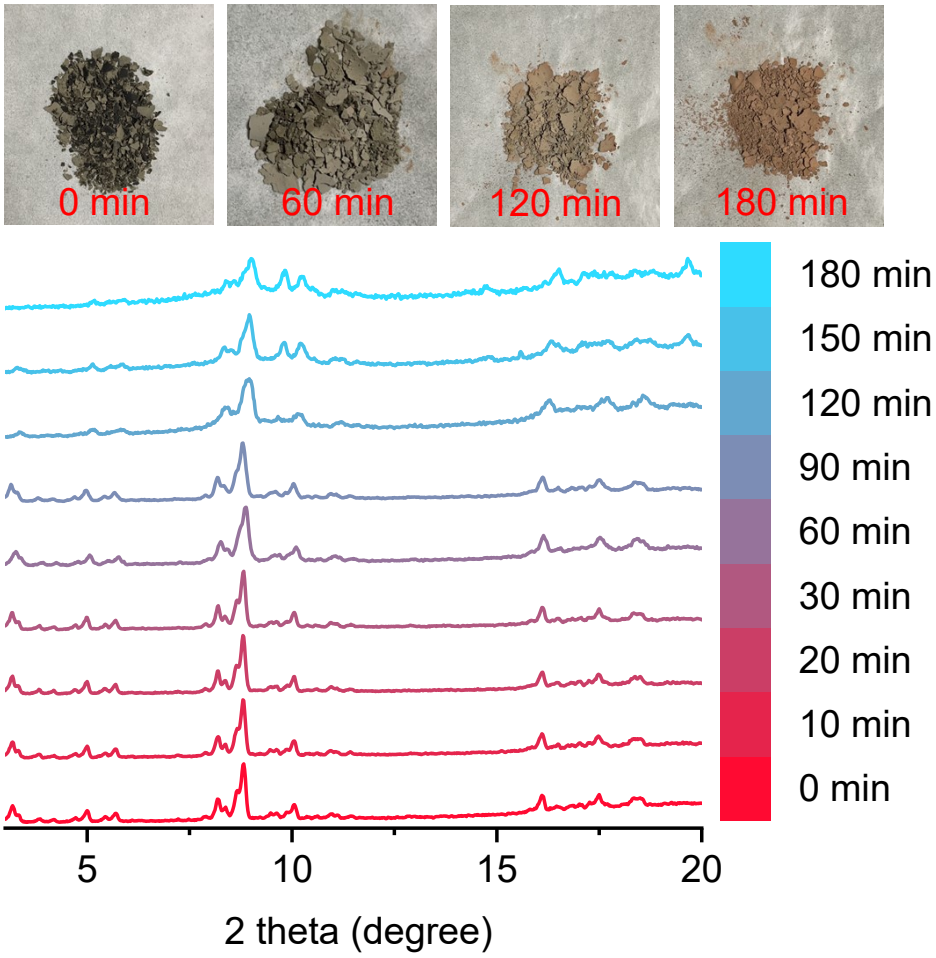

Figure S27 Air stability of MIL-101(Mn)-4-Mepy. The pictures were taken every 1 hour.

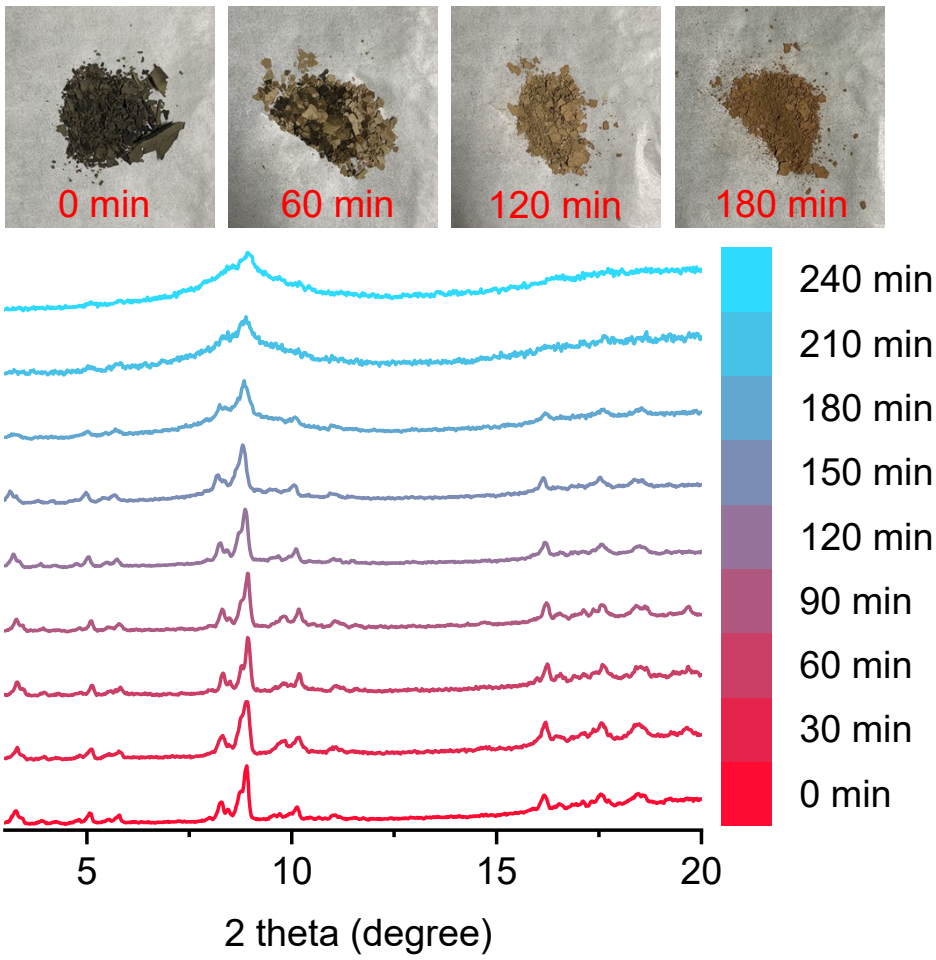

Figure S28 Air stability of MIL-101(Mn)-4-tBupy. The pictures were taken every 1 hour.

12.2 Thermalstability – TGA test

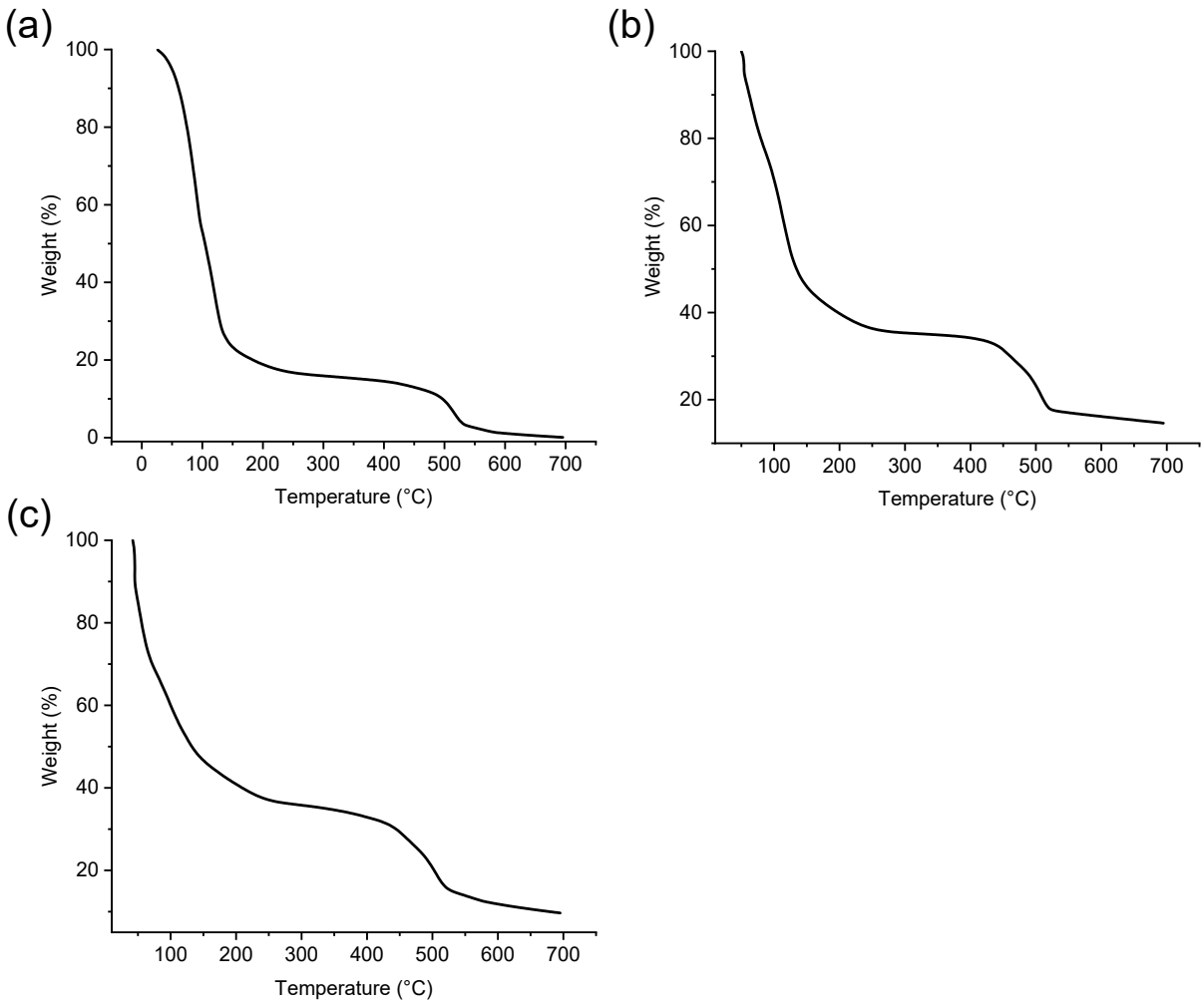

Figure S29 TGA curves of (a) MIL-101(Mn)-py, (b) MIL-101(Mn)-4-Mepy and (c) MIL-101(Mn)-4-tBupy. Note: MIL-101(Mn) is unstable upon activation, thus the TGA curves of activated samples are not given.

12.3 pH stability

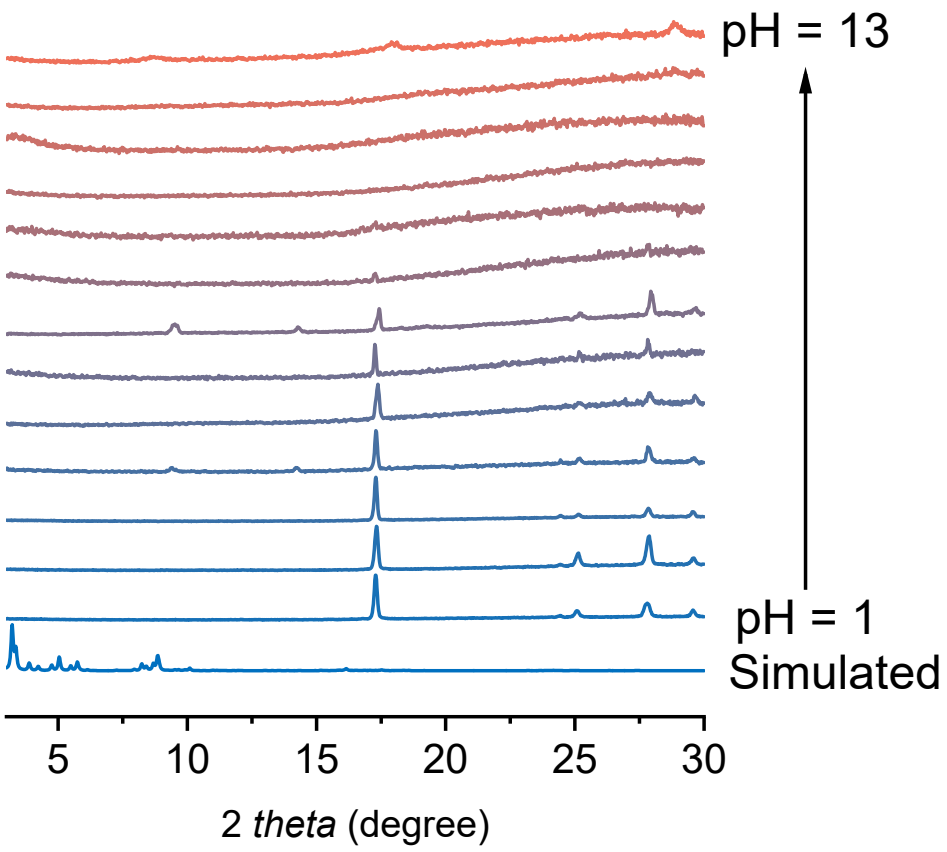

Figure S30 PXRD patterns of MIL-101(Mn) after immersing in solutions of different pH values.

13. Gas adsorption test

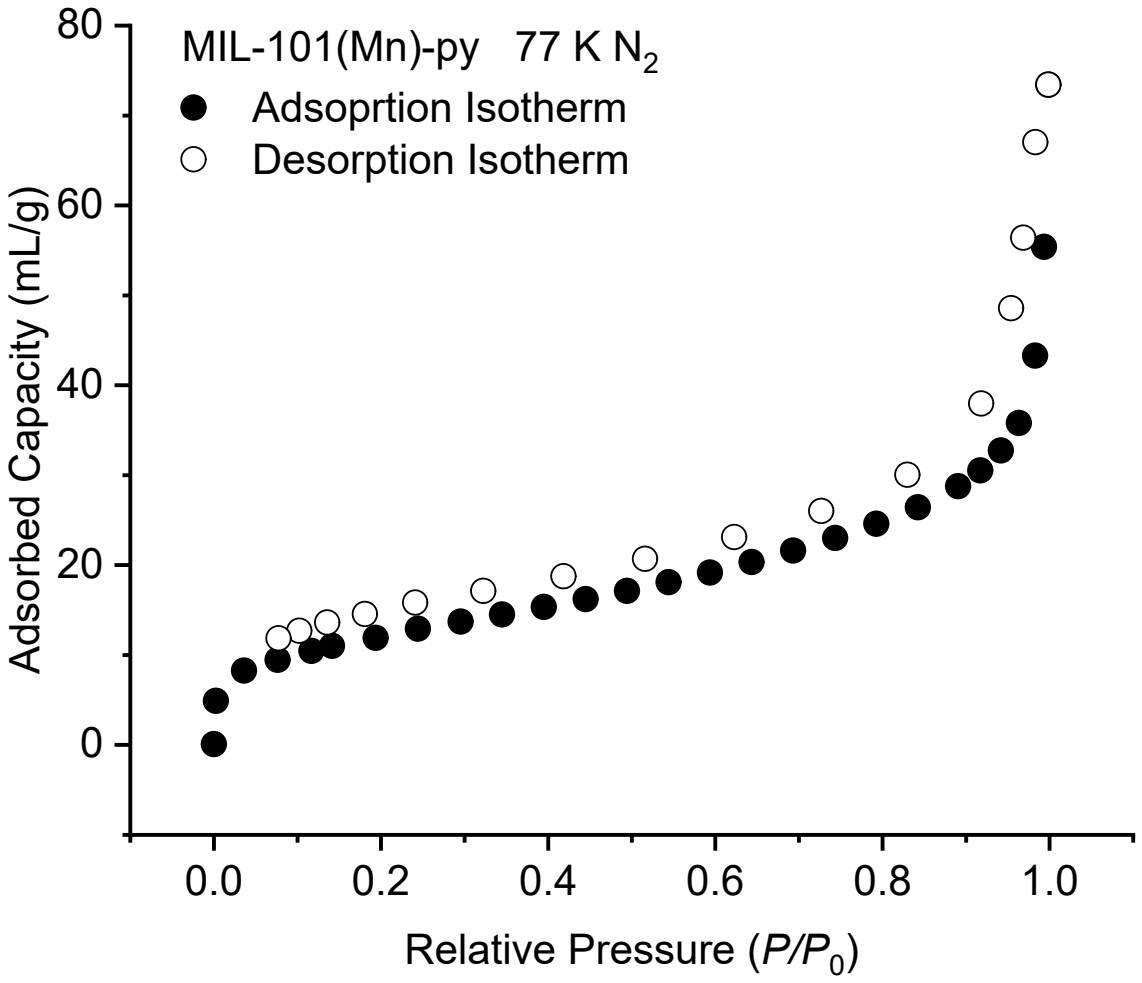

Figure S31 N_2 adsorption isotherm linear plot of MIL-101(Mn)-py at 77 K.

The low N_2 adsoprtion capacity and BET surface area of desolvated MIL-101(Mn) indicate the framework collapse upon solvent removal, that is to say, MIL-101(Mn) is unstable under such circumstance.

14. Determing specific surface area of MIL-101(Mn)-py by dye adsorption

The calculation of specific surface area is based on the adsorption of methylene blue in liquid phase. It is calculated as follows:[14]

$$S = \frac{(C_0 - C)G}{W} \times A$$

C_0 and C stands for Initial and post-adsorption concentration of methylene blue solution. G is the mass of methylene blue solution. W represents the mass of adsorbent. A is the projection area of methylene blue.

The as-synthesized MIL-101(Mn) was soaked in acetonitrile after solvent exchange using DMF×3 and acetonitrile×3. Three batches of materials were prepared.

For the surface area measurement, 2, 3, 4, 5, 6 g of 0.1 g/L methylene blue acetonitrile solution was weighed in a 50 mL volumetric flask and dilute with acetonitrile to 50 mL, to obtain methylene blue standard solutions with concentrations of 4, 6, 8, 10, 12 ppm. The absorbance was measured at 655 nm, and plotted into a standard curve.

A moderate amount of MOF material was taken in a 10 mL centrifuge tube, and then a certain mass of 0.1 g/L methylene blue solution was injected into the centrifuge tube. After soaking for three hours, take a certain mass of supernatant in a 50 mL volumetric flask and diluted to 50 mL with acetonitrile, and measure the absorbance.

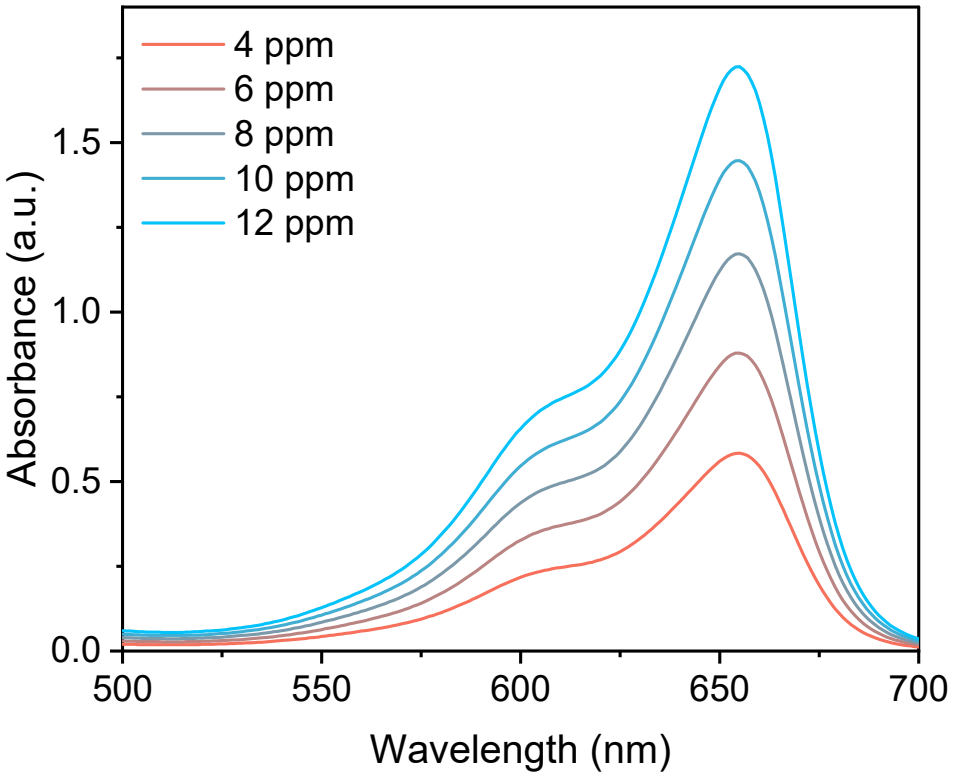

Figure S32 UV-Vis absorption spetra of methylene blue at room temperature.

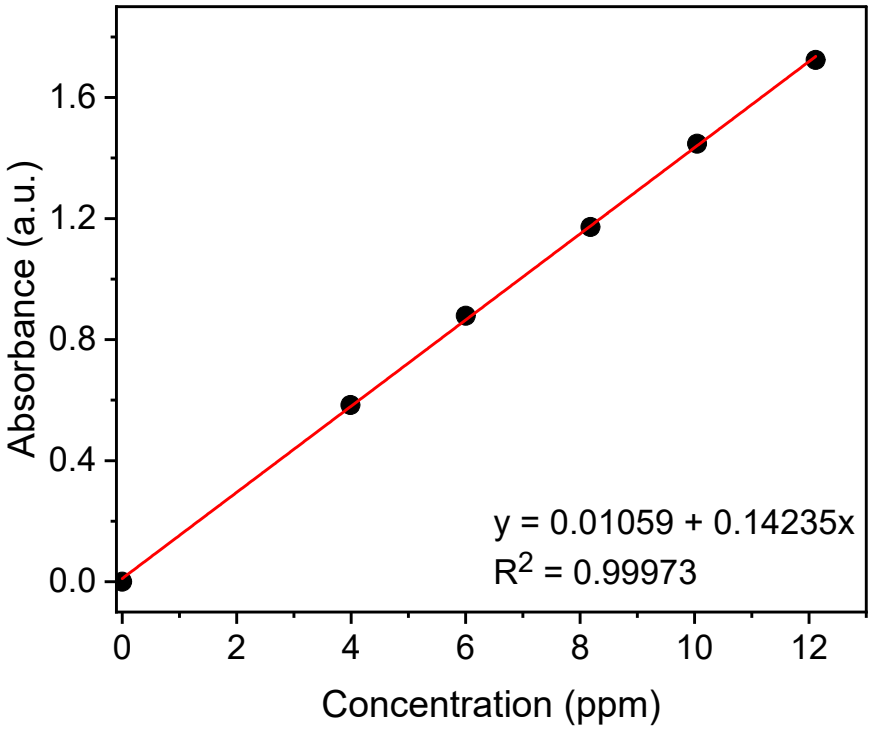

Figure S33 Standard curve of methylene blue at roomtemperature.

Table S6 Calculation result of specific surface area of MIL-101(Mn) by dye absorption method

Trial	Specific surface area calculated from five parallel experiments (m^2/g)					Average (m^2/g)	Standard Deviation(m^2/g)	C.V.
1	3024.749	2831.881	2655.216	2859.721	2943.942	2863.102	138.6251	0.04842
2	2587.516	2456.845	2427.866	2351.462	2929.445	2550.627	228.2518	0.08949
3	2806.358	2980.897	3306.765	3117.573	3475.143	3137.347	263.263	0.08391

The value is relatively lower than the reported result for MIL-101(Cr)[15] (~5900 m^2/g) and calculated result from iRASPA[13] (without coordinated pyridine: ~3579 m^2/g; with coordinated pyridine: ~3049 m^2/g), which possibly indicating the partially collapse of MIL-101(Mn) during the test.

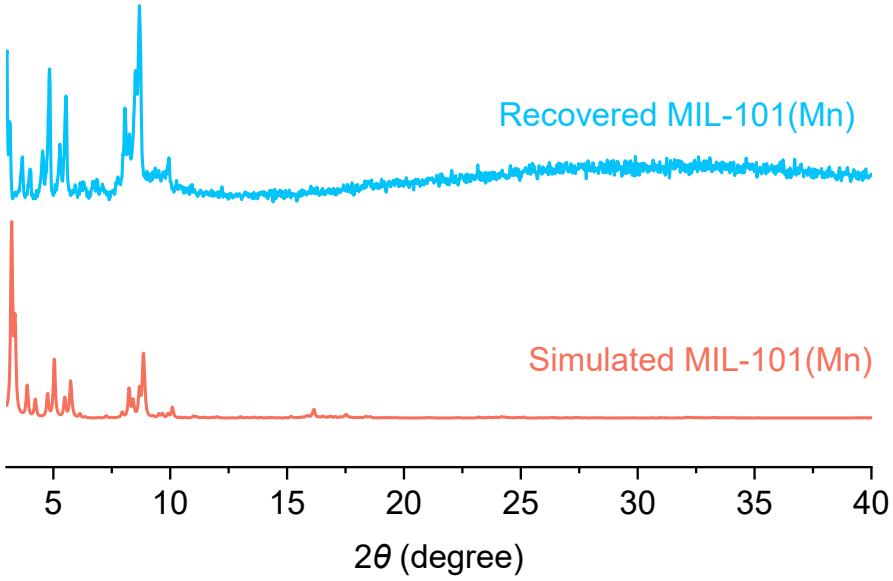

Figure S34 PXRD pattern of MIL-101(Mn) after dye adsorption test.

15. Catalysis procedure

The catalase mimetic test is based on previously reported method[16] with minor modifications.

Take 0.2 mL 8 mM TMB ethanolic solution, different volume of MOF suspension in ethanol and dilute with 0.05 M HOAc-NaOAc (pH = 5.0) to 2 mL. Place the mixture in a water bath at various temperatures and react for 30 min. Then 0.1 mL of 2 M H_2SO_4 was added to the mixed solution to terminate the reaction. Finally, the supernatant was taken using a syringe and a filter membrane, and its absorbance at 450 nm was measured. The highest point was defined as 100% relative activity. Each experiment was repeated 3 times.

16. Related MOF structures with manganese trimer SBU

No.	Structure	Manganese valence	Determination method	Reference
1	CPM-152/153/154	Not mentioned	Not mentioned	*Nat. Commun.*, 2016, **7**, 13645
2	$\{(Me_2NH_2)_2[Mn_{12}(OH)_4(abtc)_6(DMA)_6(H_2O)_6][Mn(H_2O)_4]\cdot 36H_2O\}_n$	$Mn(II)_3$	SC-XRD, Magnetic studies	*New J. Chem.*, 2019, **43**, 4226
3	JUC-102	$Mn(II)_3$	SC-XRD, dye adsorption	*Chem. Commun.*, 2012, **48**, 6010-6012
4	$(Mn_3O)_2(TCPP\text{-}M)_3$ (M = 2H, Mg, Co, Ni, Cu, Zn)	Not mentioned	Elemental analysis, XPS, but not mentioned	*J. Am. Chem. Soc.*, 2016, **42**, 13822–13825
5	MIL-100	Not able to identify detailed clusters	EPR, UV-Vis	*CrystEngComm*, 2013,**15**, 544-550
6	Mn-MIL-88, Mn-MIL-88-Me_4	$Mn(III)_2Mn(II)$	SC-XRD, magnetic studies	*Inorg. Chem.*, 2020, **12**, 8444–8450
7	Mn_3-BDC-TPP (denoted as **1**) and Mn_3-BDC-TPT (denoted as **2**)	$Mn(II)_3$ for **1** and $Mn(III)_2Mn(II)$ for **2**	SC-XRD, magnetic studies	*Cryst. Growth Des.*, 2022, **6**, 3594–3600

Supporting References

[1] M. R. Mian, U. Afrin, M. S. Fataftah, K. B. Idrees, T. Islamoglu, D. E. Freedman, O. K. Farha, *Inorg. Chem.,* 2020, **59**, 8444–8450.

[2] G. Sheldrick, *Acta Crystallogr. Sect., A* 2008, **64**, 112–122.

[3] G. Sheldrick, *Acta Crystallogr. Sect., A* 2015, **71**, 3–8.

[4] O. V Dolomanov, L. J. Bourhis, R. J. Gildea, J. A. K. Howard, H. Puschmann, *J. Appl. Crystallogr.,* 2009, **42**, 339–341.

[5] B. Zhang, S. Hao, D. Xiao, J. Wu, Y. Huang, *Mater. Des.,* 2016, **98**, 319–323.

[6] N. F. Chilton, R. P. Anderson, L. D. Turner, A. Soncini, K. S. Murray, *J. Comput. Chem.,* 2013, **34**, 1164–1175.

[7] J. P. Perdew, K. Burke, M. Ernzerhof, *Phys. Rev. Lett.,* 1997, **78**, 1396.

[8] J. P. Perdew, K. Burke, M. Ernzerhof, *Phys. Rev. Lett.,* 1996, **77**, 3865–3868.

[9] P. C. Hariharan, J. A. Pople, *Mol. Phys.,* 1974, **27**, 209–214.

[10] V. B. M. J. Frisch, G. W. Trucks, H. B. Schlegel, G. E. Scuseria, M. A. Robb, J. R. Cheeseman, G. Scalmani, G. Z. B. Mennucci, G. A. Petersson, H. Nakatsuji, M. Caricato, X. Li, H. P. Hratchian, A. F. Izmaylov, J. Bloino, O. K. J. L. Sonnenberg, M. Hada, M. Ehara, K. Toyota, R. Fukuda, J. Hasegawa, M. Ishida, T. Nakajima, Y. Honda, K. N. K. H. Nakai, T. Vreven, J. A. Montgomery, Jr., J. E. Peralta, F. Ogliaro, M. Bearpark, J. J. Heyd, E. Brothers, S. S. I. V. N. Staroverov, T. Keith, R. Kobayashi, J. Normand, K. Raghavachari, A. Rendell, J. C. Burant, J. J. J. Tomasi, M. Cossi, N. Rega, J. M. Millam, M. Klene, J. E. Knox, J. B. Cross, V. Bakken, C. Adamo, R. L. M. R. Gomperts, R. E. Stratmann, O. Yazyev, A. J. Austin, R. Cammi, C. Pomelli, J. W. Ochterski, O. F. K. Morokuma, V. G. Zakrzewski, G. A. Voth, P. Salvador, J. J. Dannenberg, S. Dapprich, A. D. Daniels, J. C. and D. J. F. J. B. Foresman, J. V. Ortiz, *Gaussian 09, Revis. A.02, Gaussian, Inc., Wallingford CT* 2009.

[11] M. Mantina, A. C. Chamberlin, R. Valero, C. J. Cramer, D. G. Truhlar, *J. Phys. Chem. A,* 2009, **113**, 5806–5812.

[12] Jerkwin, "Calculation of molecular size" , can be found under http://jerkwin.github.io/2016/06/24/%E5%88%86%E5%AD%90%E5%B0%BA%E5%AF%B8%E5%A4%A7%E5%B0%8F%E7%9A%84%E8%AE%A1%E7%AE%97/, 2016.

[13] D. Dubbeldam, S. Calero, T. J. H. Vlugt, *Mol. Simul.,* 2018, **44**, 653–676.

[14] P. G. Smith, P. Coackley, *Water Res.,* 1983, **17**, 595–598.

[15] G. Férey, C. Mellot-Draznieks, C. Serre, F. Millange, J. Dutour, S. Surblé, I. Margiolaki, *Science,* 2005, **309**, 2040–2042.

[16] X. Qi, H. Tian, X. Dang, Y. Fan, Y. Zhang, H. Zhao, *Anal. Methods,* 2019, **11**, 1111–1124.